

Cite this: *Chem. Sci.*, 2026, 17, 3908

# Virus-like particles based on plant viruses and bacteriophages: emerging strategies for the delivery of nucleic acid therapeutics

Dajeong Kim,<sup>†</sup> Bryan Duoto,<sup>†</sup> Meghana Varanasi,<sup>bcd</sup> George Goldenfeld<sup>abc</sup> and Nicole F. Steinmetz<sup>†\*</sup>

Nucleic acids have emerged as a robust modality for the treatment of various diseases that are considered undruggable in the context of small-molecule therapeutics. However, their clinical translation is hindered by the lack of safe and effective delivery across extracellular and intracellular barriers. Mammalian viral vectors and synthetic non-viral carriers have long dominated the delivery landscape, but these raise concerns about safety and immunogenicity, driving the search for alternative strategies. Recently, non-mammalian viral vectors (based on plant viruses or bacteriophages) and virus-like particles (VLPs) derived from them have gained attention as bioinspired platforms for nucleic acid drug delivery. Their well-defined architecture, scalable production, and ability to encapsulate or display drug cargoes offer versatility for drug delivery. This review highlights recent progress in the engineering of plant viruses and bacteriophages for nucleic acid delivery, emphasizing their potential as non-infectious viral scaffolds for next-generation therapeutic platforms.

Received 22nd March 2025

Accepted 13th January 2026

DOI: 10.1039/d5sc02211h

rsc.li/chemical-science

## 1. Introduction

Over the past decade, nucleic acid therapy has expanded to offer new opportunities for the prevention and treatment of infectious diseases, genetic disorders and cancer.<sup>1,2</sup> The success of mRNA-based COVID-19 vaccines brought unprecedented attention to the field, demonstrating the feasibility, scalability and rapid adaptability of nucleic acids.<sup>3</sup> More than 20 nucleic acid drugs have been approved thus far, including chemically modified antisense oligonucleotides (ASOs), *N*-acetylgalactosamine (GalNAc) ligand-conjugated small interfering RNAs (siRNAs), and adeno-associated virus (AAV)-based gene therapy.<sup>4–6</sup> For example, patisiran was the first approved siRNA therapeutic and was encapsulated in lipid nanoparticles

(LNPs),<sup>7</sup> fitusiran is a GalNAc-siRNA drug targeting anti-thrombin,<sup>8</sup> and zolgensma is an AAV-based gene therapy vector carrying the *survival motor neuron 1* transgene for the treatment of spinal muscular atrophy.<sup>8</sup> This versatile class of medicines is therefore reshaping the therapeutic landscape across a wide range of human diseases.

Progress in nucleic acid therapy has been accompanied by parallel advances in delivery strategies, including mammalian viruses and non-viral vectors.<sup>9</sup> Traditionally, mammalian viruses have been regarded as the most efficient gene delivery vehicles because this is their natural function, with lentiviral, adenoviral and AAV vectors in particular achieving efficient gene delivery, transduction, stable gene expression, and tissue specific tropism.<sup>10–12</sup> However, the limitations of such vectors include their immunogenicity,<sup>13</sup> potential integration into the host genome,<sup>14,15</sup> and cargo size restrictions.<sup>16</sup> The immune system responds to viral vectors in the same manner as live viruses, leading to safety risks for patients undergoing gene therapy.<sup>17</sup> Several fatalities have been reported during gene therapy clinical trials, including pediatric patients.<sup>18,19</sup> Moreover, pre-existing immunity against mammalian viruses reduces the transduction efficiency of viral vectors.<sup>13,20,21</sup> Concerns associated with mammalian viruses as vectors have prompted the search for safer alternatives. Non-viral delivery systems such as LNPs, polymeric carriers, and inorganic structures are less immunogenic, cannot integrate into host DNA, have a larger cargo capacity, and are easy to functionalize by chemical modification.<sup>22–24</sup> However, transfection efficiency is often poor and they tend to show physicochemical instability

<sup>a</sup>Aiiso Yufeng Li Family Department of Chemical and Nano Engineering, University of California, San Diego, La Jolla, CA 92093, USA. E-mail: nsteinmetz@ucsd.edu

<sup>b</sup>Center for Nano-ImmunoEngineering, University of California, San Diego, La Jolla, CA 92093, USA

<sup>c</sup>Shu and K. C. Chien and Peter Farrell Collaboratory, University of California, San Diego, La Jolla, CA 92093, USA

<sup>d</sup>Department of Bioengineering, University of California, San Diego, La Jolla, CA 92093, USA

<sup>e</sup>Department of Radiology, University of California, San Diego, La Jolla, CA 92093, USA

<sup>f</sup>Institute for Materials Discovery and Design, University of California, San Diego, La Jolla, CA 92093, USA

<sup>g</sup>Moores Cancer Center, University of California, San Diego, La Jolla, CA 92093, USA

<sup>h</sup>Center for Engineering in Cancer, Institute of Engineering in Medicine, University of California, San Diego, La Jolla, CA 92093, USA

<sup>†</sup> These authors contributed equally to this work.



and heterogeneity.<sup>24–26</sup> Serum-induced destabilization, inefficient endosomal escape, and rapid reticuloendothelial clearance underlie these limitations.<sup>24,27–29</sup> In addition, concerns remain regarding the immunogenicity and toxicity of the synthetic components, including ionizable lipids and cationic polymers,<sup>30,31</sup> while the lack of comprehensive *in vivo* studies for the most recent nanostructured materials creates uncertainty in terms of pharmacokinetics, long-term safety, and overall effectiveness.<sup>25,26</sup>

Naturally occurring non-mammalian viruses, particularly plant viruses and bacteriophages, overcome the disadvantages of both mammalian viruses and synthetic particles.<sup>32,33</sup> Since the discovery of tobacco mosaic virus (TMV) in 1898, structural biology has been guided by plant viruses, inspiring the field of nanobiotechnology.<sup>34,35</sup> Their biocompatibility, stability, scalable production, and robust nucleic acid encapsidation capabilities make such viruses highly attractive for biomedical

use.<sup>36–38</sup> Importantly, they are non-infectious in mammals, eliminating the safety concerns associated with human viruses.<sup>39,40</sup> Plant viruses and bacteriophages have genetically programmable capsids that can be engineered for targeting, immunomodulation, or multicomponent assembly.<sup>32,35,38,41</sup> Virus-like particles (VLPs), which resemble the parent viruses but lack the functional viral genome, can be produced on a large scale by molecular farming or bacterial fermentation because the individual coat proteins assemble spontaneously, offering a cost-effective, reproducible and stable platform for nucleic acid delivery.<sup>42,43</sup> These attributes position plant viruses and bacteriophages as the next-generation of virus-inspired nano-carriers for nucleic acid therapeutics.

In this review, we summarize the development of plant virus and bacteriophage platforms for nucleic acid therapeutics (Fig. 1). We focus on their unique molecular architectures and tunable structures, which enable the efficient encapsidation,

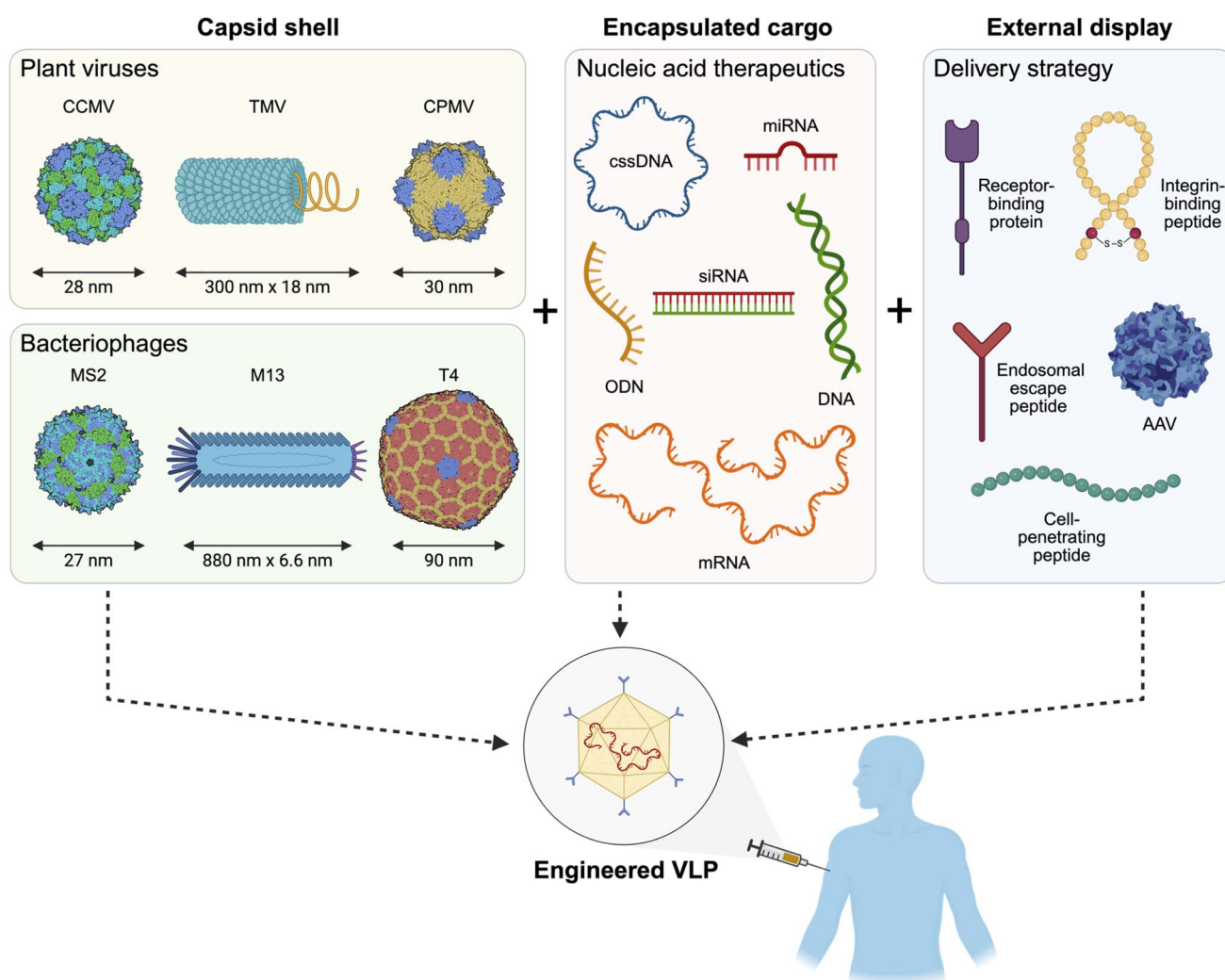


**Fig. 1** The engineering of plant viruses, bacteriophages and their derived virus-like particles (VLPs) for nucleic acid delivery by the reconstitution of capsid structures, encapsulation of nucleic acid cargo, and external display of targeting ligands and other functions. CCMV = cowpea chlorotic mottle virus, TMV = tobacco mosaic virus, CPMV = cowpea mosaic virus, cssDNA = circular single-stranded DNA, miRNA = microRNA, ODN = oligodeoxynucleotide, siRNA = short interfering RNA, mRNA = messenger RNA, AAV = adeno-associated virus. Figure was created using <https://BioRender.com>.



Table 1 Nucleic acid delivery systems based on plant viruses and their VLPs<sup>a</sup>

Vehicle	Cargo type (size)	Production method	VLP assembly	Delivery strategy	Application	Ref.
CCMV VLP	Anti-miR-181a ASO or chemically modified ASO (23 nt)	CP obtained by disassembly of CCMV from cowpea plants	<i>In vitro</i> reassembly	Naked or lipofectamine	miRNA knockdown for cancer therapy	74
	Chemically modified anti-miR-23 LNA (15 nt)	Recombinant CP expressed in <i>E. coli</i>	<i>In vitro</i> reassembly	Naked or lipofectamine	Gene silencing to treat AMD	76
	Anti-Luc siRNA (20 bp) or tRNA (80 nt)	Recombinant CP and variants (truncated CPs w/o ARD or w/ELP) expressed in <i>E. coli</i>	<i>In vitro</i> reassembly and CP cross-linking	Lipofectamine	Gene silencing, POC studies	83
	Anti-GFP or anti-FOXA1 siRNA (25 bp with 2-nt overhang)	CP obtained by disassembly of CCMV from cowpea plants or recombinant CP expressed in <i>E. coli</i>	<i>In vitro</i> reassembly	CPP (L17E M-lycotoxin peptide)	Gene silencing for cancer therapy	85
	miR-26a (n.d.)	CP obtained by disassembly of CCMV from cowpea plants	<i>In vitro</i> reassembly	Naked	Gene silencing for osteogenic differentiation of hMSCs	84
	CpG ODN1826 or ODN2138 (20 nt)	CP obtained by disassembly of CCMV from cowpea plants	<i>In vitro</i> reassembly	Naked	Cancer therapy	72
	SINV-derived mRNA cassette defective interfering RNA encoding eYFP (1800 nt)	CP obtained by disassembly of CCMV from cowpea plants	<i>In vitro</i> reassembly	Lipofectamine	Protein expression, POC studies	53
	mRNA encoding eGFP (795 nt)	CP obtained by disassembly of CCMV from cowpea plants	<i>In vitro</i> reassembly	Naked	Protein expression, POC studies	88
	mRNA encoding RdRp-eYFP or RdRp-SIINFEKL (<4000 nt)	CP obtained by disassembly of CCMV from cowpea plants	<i>In vitro</i> reassembly	Lipofectamine	mRNA vaccine, POC studies	89
CCMV VLP or BMV VLP	Anti-GFP (24 bp) or anti-Akt1 siRNA (21 bp)	CCMV and BMV obtained from cowpea and barley plants, respectively	<i>In vitro</i> reassembly	Naked	Gene silencing for cancer therapy	86
CCMV VLP or TMV VLP	mRNA encoding RdRp-eYFP (4433 nt) or RdRp-Luc (4626 nt)	Recombinant CP expressed in <i>E. coli</i>	<i>In vitro</i> reassembly	Lipofectamine (in vitro) or naked (in vivo)	Protein expression, POC studies	90
TMV VLP	mRNA encoding $\beta$ -Gal in SFV RNA cassette (13 600 nt)	CP obtained by disassembly of TMV from <i>N. benthamiana</i> plants	<i>In vitro</i> reassembly with OAS	BioTrek protein delivery agent (in vitro), RGD peptide or naked (in vivo)	Protein expression, POC studies	107
	mRNA encoding eGFP in FHV RNA cassette (3800 nt)	Recombinant VLPs produced in <i>N. benthamiana</i> plants	<i>In vitro</i> reassembly or <i>in planta</i> assembly with OAS	Naked	Protein expression, POC studies	109
	mRNA encoding RdRp-mutated E7 protein (4010 nt)	CP obtained by disassembly of TMV from <i>N. benthamiana</i> plants	<i>In vitro</i> reassembly with OAS	Lipofectamine	mRNA vaccine for therapeutics, cancer vaccination	113
	mRNA encoding RdRp-RBD (4100 nt)	CP obtained by disassembly of TMV from <i>N. benthamiana</i> plants	<i>In vitro</i> reassembly with OAS	Lipofectamine	mRNA vaccine for COVID-19 vaccination	54



Table 1 (Contd.)

Vehicle	Cargo type (size)	Production method	VLP assembly	Delivery strategy	Application	Ref.
CPMV VLP	mRNA encoding eGFP (1400 nt)	Recombinant VLPs produced in <i>N. benthamiana</i> plants by agroinfiltration	<i>In planta</i> assembly	HER2-targeting Affimer	Protein expression, POC studies	129
PVX VLP	ssRNA (1400–7600 nt) Full-length or fragmented viral RNA (250–6400 nt), mRNA encoding eGFP (870 nt), or circular RNA (2282 nt) CpG ODN (20 nt)	Recombinant VLPs produced in <i>N. benthamiana</i> plants by agroinfiltration CP obtained by disassembly of PVX from <i>N. benthamiana</i> plants	<i>In planta</i> assembly <i>In vitro</i> reassembly with SL1	— Lipofectamine	Therapeutic ssRNA packaging, POC studies Protein expression, POC studies	130 131
PhMV VLP		Recombinant CP expressed in <i>E. coli</i>	<i>In vitro</i> loading to VLP	Naked	Cancer therapy	158

<sup>a</sup> Abbreviations in table : AMD (age-related macular degeneration), ARD (arginine-rich binding domain), ASO (antisense oligonucleotide),  $\beta$ -Gal ( $\beta$ -galactosidase), c-MET (cellular mesenchymal epithelial transition), CP (coat protein), CPP (cell-penetrating peptide), eGFP (enhanced green fluorescent protein), ELP (elastin-like polypeptide), eYFP (enhanced yellow fluorescent protein), FHV (Flock House virus), GFP (green fluorescent protein), HER2 (human epidermal growth factor receptor 2), hMSC (human mesenchymal stem cell), LNA (locked nucleic acid), Luc (luciferase), n.d. (not denoted), OAS (origin of assembly sequence), ODN (oligodeoxynucleotide), POC (proof-of-concept), RdRp (RNA-dependent RNA polymerase), RBD (receptor-binding domain), SINV (Sindbis virus), SL1 (stem loop 1), VLP (virus-like particle; devoid of viral genome).

protection and transfer of nucleic acid cargoes. Furthermore, we highlight their emerging potential as safe, scalable and multifunctional delivery vehicles in mammals. We also discuss their immunogenicity and consider potential safety issues that must be addressed to ensure successful clinical translation.

## 2. Non-infectious viral vectors for nucleic acid delivery

Plant viruses and bacteriophages are natural, self-assembling nanostructures whose native hosts are non-mammalian organisms. Unlike mammalian viral vectors, they are non-infectious to mammalian cells but nevertheless offer a defined and genetically programmable capsid architecture as an ideal template for nucleic acid encapsulation.<sup>44</sup> Moreover, their self-assembled protein shells are monodisperse and structurally precise, including icosahedral, rod-like and filamentous geometries. Their assembly is primarily driven by electrostatic and steric interactions between coat proteins (CPs) and the viral genome, which enables controllable *in vitro* reconstitution and loading with heterologous nucleic acid cargoes. Furthermore, facile disassembly and reassembly allow the encapsulation and protection of diverse nucleic acid cargoes including messenger RNA (mRNA), siRNA, microRNA (miRNA), ASOs and DNA (Fig. 1).<sup>45</sup>

Plant viruses possess several key advantages as delivery vehicles for nucleic acids. First, their inability to replicate in mammalian cells offers intrinsic safety.<sup>46,47</sup> Second, production is highly scalable and cost-effective by molecular farming in plants or heterologous expression in bacteria.<sup>48,49</sup> For example, plant viruses and VLPs can be produced with a yield of ~5 g per kg of infected leaves or up to ~7 g per kg of total protein in cultures of *Escherichia coli*.<sup>48,50–52</sup> Third, their ability to encapsidate a nucleic acid genome allows the efficient packaging of heterologous nucleic acid cargoes, providing high loading capacity and protection from enzymatic degradation.<sup>53,54</sup> Fourth, they demonstrate excellent long-term stability, maintaining structural integrity and therapeutic efficacy when stored in infected plant tissues or as purified particles.<sup>55,56</sup> Fifth, plant viruses are biocompatible and stable in serum-containing media, which offers a particular advantage over many synthetic nanoparticles.<sup>57</sup> Finally, their surfaces can be engineered by genetic and chemical functionalization, enabling the display of targeting ligands, imaging probes, or immunogenic antigens.<sup>58,59</sup>

Similarly, bacteriophages are regarded as biologically safe materials due to their inability to infect or replicate in mammalian hosts. They are produced in bacteria at exceptionally high titers of up to  $\sim 1.2 \times 10^{16}$  plaque-forming units (PFU) per mL in a 5-L batch, enabling industrial-scale production.<sup>60</sup> Like plant viruses, bacteriophages are remarkably stable during storage, remaining intact for extended periods without the need for ultralow-temperature preservation.<sup>61–63</sup> Filamentous bacteriophages such as M13 have been widely used in phage display technologies to present peptide or protein libraries on their surface.<sup>64</sup> Bacteriophage T4 has a DNA cargo

capacity of up to  $\sim 170$  kbp, which is packaged by an ATP-driven motor.<sup>65</sup> With comprehensive insights into their structure and genome-packaging mechanisms, bacteriophages are amenable to rational customization of both internal and external surfaces, allowing the design of multifunctional delivery systems.

The structural predictability, modular design and programmable reassembly of plant viruses and bacteriophages make them highly versatile as scaffolds for the construction of tailored nanocarriers with diverse morphologies. However, they lack inherent tropism for mammalian cells, which is needed for the intracellular delivery of nucleic acids. Research has therefore focused on improving their transduction efficiency as well as establishing cargo-specific encapsulation strategies while retaining their intrinsic advantages of biosafety, scalability and programmability. Below, we discuss the characteristics of plant viruses and bacteriophages that position them as ideal scaffolds for next-generation nucleic acid delivery platforms (Fig. 1). Representative studies of nucleic acid drug delivery by plant viruses and bacteriophages are summarized in Tables 1 and 2, respectively.

### 3. Plant viruses as vehicles for nucleic acid delivery

#### 3.1. The cowpea chlorotic mottle virus system

Cowpea chlorotic mottle virus (CCMV) is a member of the family Bromoviridae and has a positive-sense multipartite single-stranded RNA (ssRNA) genome<sup>66</sup> encapsulated within an icosahedral capsid 28 nm in diameter and 3 nm thick, comprising 180 CPs arranged with  $T = 3$  symmetry.<sup>67</sup> The production of CCMV is scalable in black-eyed pea plants, with yields of 0.5–1 g kg<sup>-1</sup> leaf tissue,<sup>52</sup> but the CCMV CP can also be produced in bacteria with yields of up to 2.6 g L<sup>-1</sup>.<sup>68</sup> CCMV disassembles and reassembles under specific buffer conditions (pH and salt concentration) without the need for initiation sequences, enabling the formation of empty VLPs based on strong CP–CP interactions (Fig. 2a).<sup>45,69</sup> During assembly, heterologous RNA can be packaged by electrostatic interactions with CPs (Fig. 2a).<sup>70–72</sup> RNA encapsidation is a length-dependent, cooperative process, so assembly with ssRNAs shorter than the viral genome requires the co-packaging of additional RNAs to achieve fully ordered VLPs.<sup>71,73</sup> Even naked RNA anti-sense oligonucleotides (ASOs) and chemically modified RNA ASOs can be encapsulated into CCMV VLPs and protected by CPs.<sup>74</sup> For example, VLPs containing anti-miR-181a ASOs achieved the efficient knockdown miR-181a in three cancer cell lines, effectively blocking their proliferation and inhibiting their invasiveness.<sup>74</sup>

Similarly, 15-nt locked nucleic acids (LNAs) were loaded into CCMV VLPs enabling the silencing of miR-23 as a treatment for age-related macular degeneration (AMD).<sup>76</sup> LNAs are bicyclic oligonucleotide analogs with a methylene bridge linking the 2' oxygen and 4' carbon to improve binding affinity.<sup>77</sup> The VLPs achieved a loading efficiency of 87% for anti-miR-23 LNAs, remaining at 79% after further stabilization by cross-linking CPs using 3,3'-dithiobis(sulfosuccinimidylpropionate)

(DTSSP). The cross-linked VLPs improved capsid stability, allowing miR-23 knockdown even in the absence of a transfection agent.<sup>76</sup> Notably, the chemical modification of nucleobases has a negligible impact on the encapsulation process.<sup>72,74,76</sup>

The assembly of VLPs based on electrostatic interactions between CCMV CPs also allowed the encapsulation of single-stranded DNA (ssDNA) (Fig. 2a and b).<sup>72,75,76,78,79</sup> The assembly of CCMV VLPs containing ssDNA requires a minimum length of 14 nt, but longer DNAs ( $\sim 20$  nt) promote faster and more efficient packaging.<sup>80</sup> The encapsulation of CpG oligonucleotides (CpG ODNs) into CCMV VLPs triggered antitumor responses (Fig. 2c).<sup>72</sup> CpG ODNs are immunostimulatory molecules that activate innate immune cells by signaling through Toll-like receptor 9 (TLR9).<sup>81,82</sup> VLPs containing CpG ODNs were structurally similar to native CCMV but enabled delivery to (and the subsequent activation of) tumor-associated macrophages.<sup>72</sup>

CCMV has also been used to deliver regulatory miRNAs and siRNAs.<sup>83–86</sup> CCMV VLPs can encapsulate 22-bp miRNAs at a capacity of  $\sim 16$  molecules per VLP.<sup>84</sup> The resulting miR-26a-carrying VLPs were internalized by human mesenchymal stem cells (hMSCs) and efficiently released their miRNA cargo into the cytoplasm, promoting osteogenic differentiation comparable to that achieved with Lipofectamine-mediated delivery.<sup>84</sup> A 25-bp siRNA targeting eGFP could also be assembled into CCMV VLPs with CP conjugated to the L17E variant of M-lycotoxin, a cell penetrating peptide (CPP).<sup>85</sup> The VLPs displaying L17E outperformed native VLPs, enabling transfection reagent-free delivery and gene silencing.<sup>85</sup>

Interestingly, the shape of assembled CCMV CP nanostructures can be altered by the type of nucleic acid cargo. Whereas ssRNA, short double-stranded RNA (dsRNA) and ssDNA make icosahedral particles, long double-stranded DNA (dsDNA) redirects their assembly into tubular nanostructures (Fig. 2d and e).<sup>75,78,79</sup> The tube length can be controlled by altering the dsDNA : CP ratio, as shown with dsDNA molecules of 1, 7.3 and 23 kbp.<sup>78</sup> The tube has a uniform diameter of 17 nm, in some cases with hemispherical caps showing  $T = 1$  symmetry.<sup>79</sup> The packaging of a 563-bp dsRNA yielded long, curved nanorods with a diameter of  $\sim 21$  nm.<sup>87</sup> The ssDNA-containing icosahedral VLPs were internalized mainly by clathrin-mediated endocytosis, whereas dsDNA-containing rods were taken up by micropinocytosis, highlighting the structure-dependent cell uptake of VLPs.<sup>75</sup> These findings emphasize the flexibility and versatility of the CCMV-mediated nucleic acid delivery system.

The intrinsic ability of CCMV to encapsidate the native  $\sim 3.1$ -kb genome implies the potential to package even longer heterologous nucleic acids.<sup>53,88,89</sup> CCMV VLPs have been shown to encapsulate an *in vitro* transcribed 1800-nt heterologous RNA cassette derived from Sindbis virus (SINV) (Fig. 2f).<sup>53</sup> While retaining the 5' and 3' untranslated regions (UTRs) as *cis*-acting elements for replication, the nonstructural coding region of SINV was modified to express the enhanced yellow fluorescent protein (eYFP), creating a defective-interfering RNA template (DI-eYFP).<sup>53</sup> In proof-of-concept experiments, CCMV VLPs could be induced to express eYFP following Lipofectamine-mediated



Table 2 Nucleic acid delivery systems based on bacteriophages<sup>a</sup>

Vehicle	Cargo type (size)	Production method	VLP assembly	Delivery strategy	Application	Ref.
MS2 VLP	mRNA encoding HIV-1 Gag (1529 nt)	Recombinant VLPs produced in yeast	<i>In situ</i> RNA packaging with C variant <i>pac</i> site	—	mRNA vaccine, POC studies	174
	mRNA encoding PAP-GM-CSF (1566 or 1581 nt)	Recombinant VLPs produced in yeast	<i>In situ</i> RNA packaging with C variant <i>pac</i> site	—	Cancer vaccine	177
	Pre-miR-146a (93 nt)	Recombinant VLP with miRNA produced in <i>E. coli</i>	<i>In situ</i> RNA packaging with C5 variant <i>pac</i> site	TAT peptide	Gene silencing, POC studies	172 and 177
	Pre-miR-146a (93 nt)	Recombinant VLP with miRNA produced in <i>E. coli</i>	<i>In situ</i> RNA packaging with C5 variant <i>pac</i> site	TAT peptide	Gene silencing to treat SLE	178
	Pre-miR-146a (n.d.)	Recombinant VLP with miRNA produced in <i>E. coli</i>	<i>In situ</i> RNA packaging with C5 variant <i>pac</i> site	TAT peptide	Gene silencing to inhibit osteoclastogenesis	179
	miR-21-sponge (142 nt) or pre-miR-122-miR-21-sponge (277 nt)	Recombinant VLP produced in <i>E. coli</i>	<i>In situ</i> RNA packaging with <i>pac</i> site	EGFR ligand (GE11)	Gene silencing for cancer therapy	180
	Pre-miR-122 (~100 nt)	Recombinant VLP with miRNA produced in <i>E. coli</i>	<i>In situ</i> RNA packaging with <i>pac</i> site	TAT peptide	Gene silencing for cancer therapy	181
	Anti-Bcl2 siRNA (19 nt - 21 bp)	Recombinant CP produced in <i>E. coli</i>	<i>In vitro</i> reassembly with <i>pac</i> site	Human transferrin	Gene silencing for cancer therapy	183
	Anti-cyclin siRNA cocktails (n.d.)	Recombinant CP in <i>E. coli</i>	<i>In vitro</i> reassembly w/o <i>pac</i> site	HCC-specific peptide (SP94) and fusogenic peptide	Gene silencing for cancer therapy	184
	ODN against p120 (20 nt)	Recombinant CP produced in <i>E. coli</i>	<i>In situ</i> RNA packaging with <i>pac</i> site	Transferrin	Gene silencing for cancer therapy	185
Q $\beta$ VLP	ODN (20 nt) or mRNA (770 nt)	Recombinant SpyTag-VLPs produced in <i>E. coli</i> or CP obtained by disassembly of VLPs	<i>In vitro</i> packaging by diffusion into VLP (ODN) or <i>in vitro</i> reassembly with <i>pac</i> site (mRNA)	—	ODN and mRNA delivery, POC studies	190
	CpG ODN (19–30 nt)	Recombinant VLPs produced in <i>E. coli</i>	<i>In vitro</i> packaging through diffusion into VLP	—	Cancer vaccine, POC studies	200 and 202
	B-type CpG ODN (20 nt)	Recombinant CP produced in <i>E. coli</i>	<i>In vitro</i> packaging by diffusion into VLP	—	Cancer vaccine	198 and 201
	A-type CpG ODN (30 nt); CMP-001	Recombinant CPs produced in <i>E. coli</i>	<i>In vitro</i> reassembly	—	Cancer therapy	203–206
	Bacterial RNA (n.d.)	Recombinant VLPs produced in <i>E. coli</i>	<i>In situ</i> packaging of bacterial RNA with Q $\beta$ CP binding hairpin	—	Vaccine for viral infection	207 and 208
	c-MET RNAi scaffold (~96 nt)	Recombinant VLPs produced in <i>E. coli</i>	<i>In situ</i> packaging with Q $\beta$ CP binding hairpin	CPP, ApoE peptide	Gene silencing for cancer therapy	209
	Anti-Luc siRNA (18 bp)	CP obtained by disassembly of recombinant Q $\beta$ VLP produced in <i>E. coli</i>	<i>In vitro</i> reassembly	TPP peptide	Gene silencing for cancer therapy, POC studies	210
	Anti-EGFR siRNA, miRNA Let-7g and broccoli aptamer on 3WJ RNA (237 nt)	Recombinant VLPs produced in <i>E. coli</i>	<i>In situ</i> packaging with Q $\beta$ CP binding hairpin	TAT peptide	Gene silencing for cancer therapy	211

Table 2 (Contd.)

Vehicle	Cargo type (size)	Production method	VLP assembly	Delivery strategy	Application	Ref.
M13 VLP	DNA encoding eGFP or $\beta$ -Gal (n.d.)	Recombinant VLPs produced in <i>E. coli</i> by phagemid and helper phage	<i>In situ</i> DNA packaging	FGF2, EGF, or transferrin	Gene delivery, POC studies	215
	DNA encoding GFP (2500 nt), GFP-TET (4400 nt) or Luc (3100 nt)	Recombinant VLPs produced in <i>E. coli</i> by mini-phagemid and helper phage	<i>In situ</i> DNA packaging without bacterial backbone	—	Gene delivery, POC studies	220
	DNA encoding Luc or GFP (n.d.)	Recombinant VLPs produced in <i>E. coli</i> by mini-phagemid and helper phage	<i>In situ</i> DNA packaging without bacterial backbone	EGF peptide	Targeted gene delivery, POC studies	221
	DNA encoding membrane-bound Fc (2384 nt) or various lengths (221–6133 nt)	Recombinant VLPs produced in <i>E. coli</i> by mini-phagemid and helper phage	<i>In situ</i> DNA packaging without bacterial backbone	EGF	Gene delivery for cancer therapy	222
M13 AAVP	DNA encoding GFP (2429 nt) or various lengths (285–2429 nt)	Recombinant VLPs produced in <i>E. coli</i> by mini-phagemid and helper phage	<i>In situ</i> DNA packaging without bacterial backbone	CTX peptide	Gene delivery for cancer therapy, POC studies	223
	DNA containing canonical CpG hexamers with various lengths (721–6261 nt)	Recombinant VLP produced in <i>E. coli</i> by plasmid and helper phage	<i>In situ</i> DNA packaging without bacterial backbone	—	Cancer vaccine	232
	DNA encoding GFP, Luc, or HSVtk flanked by AAV ITRs (~13 200 nt)	Recombinant AAVPs produced in <i>E. coli</i>	<i>In situ</i> DNA packaging	RGD-4C peptide	Gene delivery for cancer therapy	224
	DNA encoding eGFP flanked by AAV ITRs (~10 500 nt)	Recombinant AAVPs produced in <i>E. coli</i>	<i>In situ</i> DNA packaging	RGD8 peptide	Tissue engineering material and gene delivery, POC studies	225
M13	DNA encoding Luc flanked by AAV ITRs (n.d.)	Recombinant AAVPs produced in <i>E. coli</i>	<i>In situ</i> DNA packaging	RGD-4C and endosome-escape peptide (H5WYG, INF7 or PC1)	Gene delivery for cancer therapy, POC studies	226
	DNA encoding TNF $\alpha$ flanked by AAV ITRs (n.d.)	Recombinant AAVPs produced in <i>E. coli</i>	<i>In situ</i> DNA packaging	RGD-4C and endosome-escape peptide (H5WYG)	Gene delivery for cancer therapy	227
T4 VLP	DNA encoding IL-12, IL-15, or TNF $\alpha$ flanked by AAV ITRs (~5378 nt)	Recombinant TPA particles produced in <i>E. coli</i> by TPA plasmid and helper phage	<i>In situ</i> DNA packaging without phage genome	RGD-4C	Gene delivery for cancer therapy	228 and 229
	DNA encoding Luc or HSVtk (n.d.)	Recombinant M13 phages expressed in <i>E. coli</i>	<i>In situ</i> DNA packaging	RGD-4C, cationic polymers	Gene delivery for cancer therapy	234
T4 VLP	DNA encoding luciferase, GFP (n.d.) or with various lengths (2.3–170 kbp)	Recombinant Soc- and Hoc-mutated, empty T4 heads produced in <i>E. coli</i>	<i>In vitro</i> DNA packaging using packaging motor	CPP (TAT or Antp), DEC205 mAb, or CD40 ligand	Gene therapy, POC studies	65





Table 2 (Contd.)

Vehicle	Cargo type (size)	Production method	VLP assembly	Delivery strategy	Application	Ref.
T4 phage	DNA encoding SARS-CoV-2 full spike protein (6.5 kbp), RBD (2.7 kbp) or nucleoprotein (1.3 kbp)	Recombinant T4 particle produced in <i>E. coli</i> by CRISPR-mediated genome editing	<i>In situ</i> DNA packaging	—	SARS CoV-2 vaccine	241
	DNA encoding sfGFP or ClpB (n.d.)	Recombinant T4 particle produced in <i>E. coli</i>	<i>In situ</i> DNA packaging through T4-specific promoter	—	Gene delivery for reprogramming gut bacterium	244
	Plasmid DNA encoding EPO-Keap1 on the surface (2832 bp)	Recombinant Soc-mutated T4 particle produced in <i>E. coli</i>	<i>In vitro</i> DNA loading through electrostatic interaction with PLL-modified phage	—	Gene delivery for cancer therapy	245
T4 AAVP	DNA encoding Luc or HA flanked by AAV ITRs (~6.2 kbp)	Recombinant empty T4 heads produced in <i>E. coli</i>	<i>In vitro</i> DNA packaging using packaging motor	AAV particles	DNA vaccine	243
	DNA encoding dystrophin-Luc-Pac-mCherry polygene (20 kbp), Pac (6.6 kbp), Pac-SARS-CoV-2 S-ecto (11.1 kbp), mCherry, LacO-Luc, Luc, GFP flanked by AAV ITRs (n.d.) or gRNA, siRNA, mRNA (n.d.) on the surface	Recombinant empty T4 heads produced in <i>E. coli</i>	<i>In vitro</i> DNA packaging using packaging motor or <i>in vitro</i> RNA displaying by RNP with Cas9-fused Soc	RGD, TAT, Cas9, Cpf1, Cre, $\beta$ -Gal, GFP and positively charged lipid	Combinatory delivery of DNA, RNA, and proteins, POC studies	242
$\lambda$ phage	DNA encoding $\beta$ -gal (n.d.) inserted into phage genome	Recombinant $\lambda$ phage produced in <i>E. coli</i>	<i>In situ</i> DNA packaging	RGD peptide	Gene delivery, POC studies	253
	DNA encoding GFP (n.d.) inserted into phage genome	Recombinant $\lambda$ phage produced in <i>E. coli</i>	<i>In situ</i> DNA packaging	Pb protein or peptide of adenovirus	Chimeric particles for gene transfer	254
	DNA encoding HBsAg (n.d.) inserted into phage genome	Recombinant $\lambda$ phage produced in <i>E. coli</i>	<i>In situ</i> DNA packaging	—	DNA vaccine	256–258
	DNA encoding GFP (~700 bp) or E7 (~300 bp) inserted into phage genome	Recombinant $\lambda$ phage produced in <i>E. coli</i>	<i>In situ</i> DNA packaging	—	Gene delivery for cancer therapy	259
PP7 VLP	DNA encoding apoptin (396 bp) inserted into phage genome	Recombinant $\lambda$ phage produced in <i>E. coli</i>	<i>In situ</i> DNA packaging	—	Gene delivery for cancer therapy	260
	Pre-miR-23b (136 nt)	Recombinant PP7 VLPs produced in <i>E. coli</i>	<i>In situ</i> DNA packaging with <i>pac</i> site	TAT peptide	Gene silencing for cancer therapy, POC studies	264

<sup>a</sup> Abbreviations in table: 3WJ (three-way junction), AAV (adeno-associated virus), AAVP (adeno-associated virus and phage), ApoEP (apolipoprotein E peptide), ClpB (serine protease inhibitor B1a), Cre (Cre recombinase), CP (coat protein), CPP (cell-penetrating peptide), CTX (chlorotoxin), EGF (epidermal growth factor), EGFR (EGF receptor), FGF (fibroblast growth factor), GM-CSF (granulocyte macrophage colony-stimulating factor), HA (influenza virus hemagglutinin), ITR (inverted terminal repeat), HCC (hepatocellular carcinoma), LacO (lac operator sequence), n.d. (not denoted), Pac (puromycin resistant gene), *pac* (packaging site), PAP (prostate-extended antigen), RNAi (RNA interference), RNP (ribonucleoprotein), S-ecto (spike ectodomain gene), sfGFP (super-fold GFP), SLE (systemic lupus erythematosus), Soc/Hoc (small/highly immunogenic outer capsid proteins), TET (tetracycline resistance), TPA (transmorphic phage/AAV), TPP (triphenylphosphonium), Pb (penton base), PLL (poly-L-lysine), VLP (virus-like particle; devoid of viral genome).

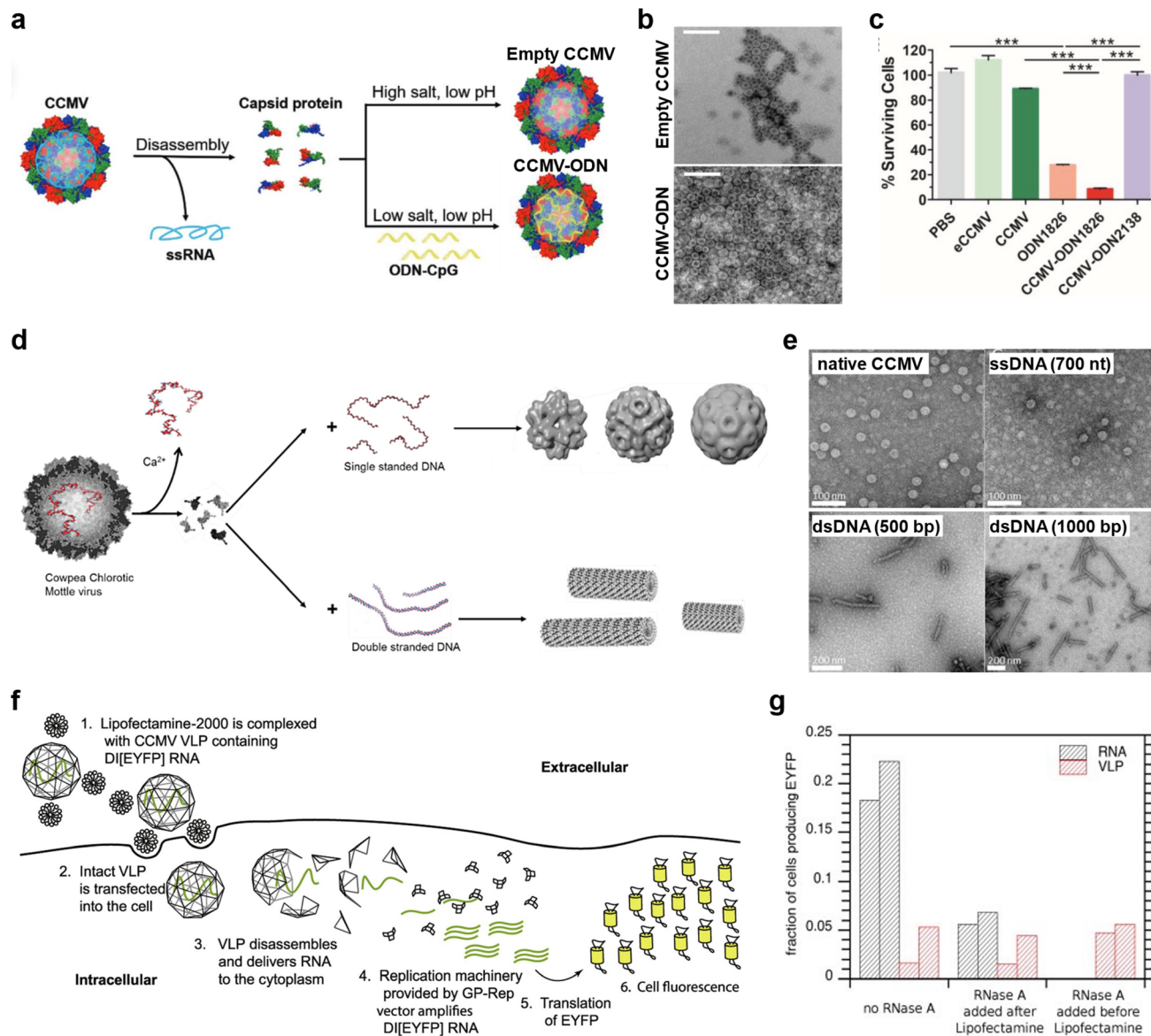


Fig. 2 Applications of CCMV VLPs for delivery of nucleic acid therapeutics. (a) Schematic showing the disassembly and reassembly of empty CCMV VLPs and CpG oligonucleotide (ODN)-encapsulating CCMV VLPs (CCMV-ODN). (b) Transmission electron microscopy (TEM) micrographs of empty CCMV and CCMV-ODN. Scale bars: 100 nm. (c) Survival of CT26 cells after co-culture with bone marrow-derived macrophages (BMDMs) stimulated with the ODN or VLPs showing anti-tumor activity of stimulated BMDMs. Reproduced from ref. 72 with permission from John Wiley and Sons, copyright 2020. (d) Encapsulation of ssDNA or dsDNA into CCMV VLP by assembly with CCMV CPs. (e) TEM micrographs of CCMV VLPs encapsulating DNA strands of different length or structures, showing the resulting morphological differences among the VLPs. Reproduced from ref. 75 with permission from Elsevier, copyright 2019. (f) Lipofectamine-mediated delivery of CCMV VLPs encapsulating heterologous mRNA into mammalian cells and subsequent induction of protein expression. (g) Expression of enhanced yellow fluorescent protein (eYFP) in mammalian cells following transfection with naked mRNA (RNA) or mRNA encapsulated in CCMV VLPs (VLP). Reproduced from ref. 53 with permission from Elsevier, copyright 2013.

transfection followed by the introduction of SINV-like particles to initiate the replication of DI-eYFP (Fig. 2g).<sup>53</sup> More recently, a self-amplifying mRNA (saRNA) was encapsulated in CCMV VLPs by using RNA-dependent RNA polymerase (RdRp) to maximize and prolong protein expression.<sup>89,90</sup> CCMV CP was used to encapsulate a ~3200-nt replicon encoding Nodamura virus RdRp in conjunction with a downstream transgene, enabling a 150-fold increase in transcription compared to a non-replicating mRNA.<sup>89</sup> Further studies with a replicon

encoding the MHC class I epitope SIINFEKL as a model antigen showed that the CCMV VLP stimulated dendritic cell activation and T-cell priming.<sup>89</sup> Also, mouse footpad injections resulted in the robust expression of eYFP in the draining lymph nodes, showing that CCMV VLPs are suitable candidates for mRNA vaccine design.<sup>90</sup>

CCMV can also be used to present CP-nucleic acid hybrid origami structures.<sup>91–93</sup> For example, rectangular DNA origami has been wrapped into rolled-tube and fully coated sheet



structures *via* electrostatic interactions with increasing amounts of CP, resulting in enhanced delivery to HEK 293 cells.<sup>91</sup> Taking advantage of programmable DNA nanotechnology, the finely tuned DNA origami structures could be coated with CCMV CPs.<sup>92</sup> Although there was a preference for tubular structures such as six-helix bundles (6HB), all tested structures were successfully coated with CCMV CPs, including the toroidal 13-helix ring (13HR) and brick-like 60HB with low aspect ratio, as well as DNA-RNA hybrid 6HB.<sup>92</sup> This unique origami-coating strategy was expanded to deliver mRNA into cells.<sup>93</sup> The encapsulation of mRNA-DNA origami encoding enhanced green fluorescent protein (eGFP) by CCMV CPs conferred stability against nucleases and increased uptake efficiency without Lipofectamine, although eGFP was only expressed in the presence of Lipofectamine.<sup>93</sup>

Although Lipofectamine has been widely used for gene delivery and expression *in vivo*, more recent studies have shown that transfection agents are not required.<sup>90</sup> Further research is required to understand the trafficking of plant VLPs in cells. CCMV is taken up mainly by clathrin-mediated or caveolae-mediated endocytosis, or in some cases by micropinocytosis,<sup>75</sup> but the endolysosomal escape of VLPs and the release of RNA cargo into the cytoplasm is not fully understood. This foundational knowledge is needed to refine VLP designs and to determine whether CPPs or specific RNA release mechanisms must be included to maximize gene delivery and unlock the full potential of this gene delivery technology.

### 3.2. The tobacco mosaic virus system

TMV is a rod-shaped *Tobamovirus* with a 6.4-kb positive-sense ssRNA genome.<sup>94,95</sup> Each TMV particle is composed of 2130 identical CP subunits that form a rigid, hollow nanotube 300 nm in length and 18 nm in diameter.<sup>96</sup> The helical structure of TMV comprises 16.3 CP subunits per turn, with a pitch of 2.3 nm, forming an internal channel 4 nm in diameter.<sup>96,97</sup> Wild-type TMV can be produced in infected leaves with a yield of 1–5 g kg<sup>-1</sup> leaf tissue.<sup>50</sup> TMV VLPs encapsulating heterologous RNA can be produced *in planta* using plasmids expressing TMV CP and the heterologous RNA cargo,<sup>98</sup> in *E. coli*,<sup>51</sup> and by *in vitro* assembly from individually purified CP and RNA components, achieving assembly yields of ~60% relative to input TMV CP.<sup>54</sup> Among the limited studies available, the predominant strategy for the preparation of TMV VLPs involves the *in vitro* self-assembly of disassembled CPs and synthetic RNA templates, particularly for applications in mammals.<sup>90</sup>

The reconstitution of TMV involves the polymerization of pre-formed CP disks together with RNA.<sup>99,100</sup> The TMV genome has a 3' origin of assembly sequence (OAS) that initiates the assembly of TMV CPs using viral RNA as the template (Fig. 3a).<sup>101,102</sup> Tubular TMV VLPs can encapsulate heterologous ssRNA by direct self-assembly if an OAS-containing RNA strand is used, and the length of the tube is dependent on the length of the ssRNA (Fig. 3a and b).<sup>103–105</sup> For example, TMV CPs have been shown to encapsulate synthetic mRNA encoding chloramphenicol acetyltransferase (CAT) linked to the TMV OAS.<sup>103</sup> This non-viral 1.2-kb transcript was successfully assembled into

TMV VLPs 60 nm in length, consistent with the theoretical size.<sup>103,105</sup> The expression of CAT was confirmed in animal cells by microinjection, demonstrating that TMV VLPs are disassembled to release encapsidated foreign mRNA.<sup>103</sup> OAS-containing RNA scaffolds of different lengths allow the production of TMV VLPs with tunable aspect ratios and distinct biodistribution profiles, depending on their shape and surface coating.<sup>105</sup> In particular, a 130-nm TMV VLP coated with the integrin binding cyclic peptide RGD showed high tumor-targeting efficiency due to tumor-specific binding and enhanced diffusion.<sup>105</sup>

TMV has been used as an RNA vaccine carrying a *trans*-encapsidated viral genome cassette encoding RNA replicase and a target protein.<sup>107–109</sup> A 13.6-kb vector was developed by linking the Semliki Forest virus (SFV) replicon to a *lacZ* reporter gene and TMV OAS, which was then packaged *in vitro* with TMV CPs.<sup>107</sup> The SFV-TMV pseudovirus was 600 nm in length and enabled  $\beta$ -galactosidase ( $\beta$ -Gal) expression *in vitro*.<sup>107</sup> Successful mRNA delivery and transgene expression in C57BL/6 mice was demonstrated by  $\beta$ -Gal-specific immune responses, confirming the co-translational disassembly of pseudovirus particles.<sup>107</sup> The immune response was similar for VLPs assembled from wild-type CP or CP fused to the RGD peptide, indicating that TMV VLPs entered immune cells *in vivo*.<sup>107</sup> This result agreed with studies showing that TMV is taken up efficiently by dendritic cells and can activate dendritic cells and macrophages.<sup>110–112</sup>

More recently, TMV was also used to encapsidate the small RNA genome of Flock House virus (FHV), which is known for its rapid replication and inability to trigger apoptosis, in contrast to the 11.5-kb SFV replicon.<sup>108,109</sup> The 3.8-kb construct consisted of FHV RNA1 containing a 3.1-kb RdRp gene linked to *eGFP* and the TMV OAS. The RNA cargo was then encapsidated by *in vitro* assembly or synthesis in *Nicotiana benthamiana* plants.<sup>109</sup> Testing in mice revealed that particles assembled *in planta* elicited a stronger immune response than those assembled *in vitro*, possibly due to inefficient *in vitro* 5' capping resulting in low transgene expression.<sup>109</sup>

TMV VLPs were recently used for saRNA vaccine delivery.<sup>54,90,113</sup> A 4-kb RNA replicon cassette including the *eYFP* reporter gene and Nodamura virus RdRp gene was encapsulated efficiently, and VLPs carrying the saRNA remained stable and enabled reporter protein expression in lymph nodes following injection into mouse foot pads.<sup>90</sup> By replacing the reporter with a mutated human papillomavirus (HPV)-16 E7 oncogene, a VLP vaccine candidate was constructed for the treatment of HPV<sup>+</sup> tumors.<sup>113</sup> The VLP induced the production of E7-specific IgG and IgM, confirming an effective humoral immune response.<sup>113</sup> Additionally, the mutant E7 protein induced naïve T cells to proliferate and differentiate into E7-specific effector T cells and produce significant levels of interferon  $\gamma$  (IFN $\gamma$ ) and interleukin (IL)-4, indicating priming of the memory T cell response in vaccinated mice.<sup>113</sup> The saRNA cassette was developed as a COVID-19 vaccine by replacing the E7 oncogene with the receptor binding domain (RBD) of SARS-CoV-2 (Fig. 3c).<sup>54</sup> The resulting VLP induced the production of RBD-specific neutralizing IgG antibodies (Fig. 3d).<sup>54</sup>



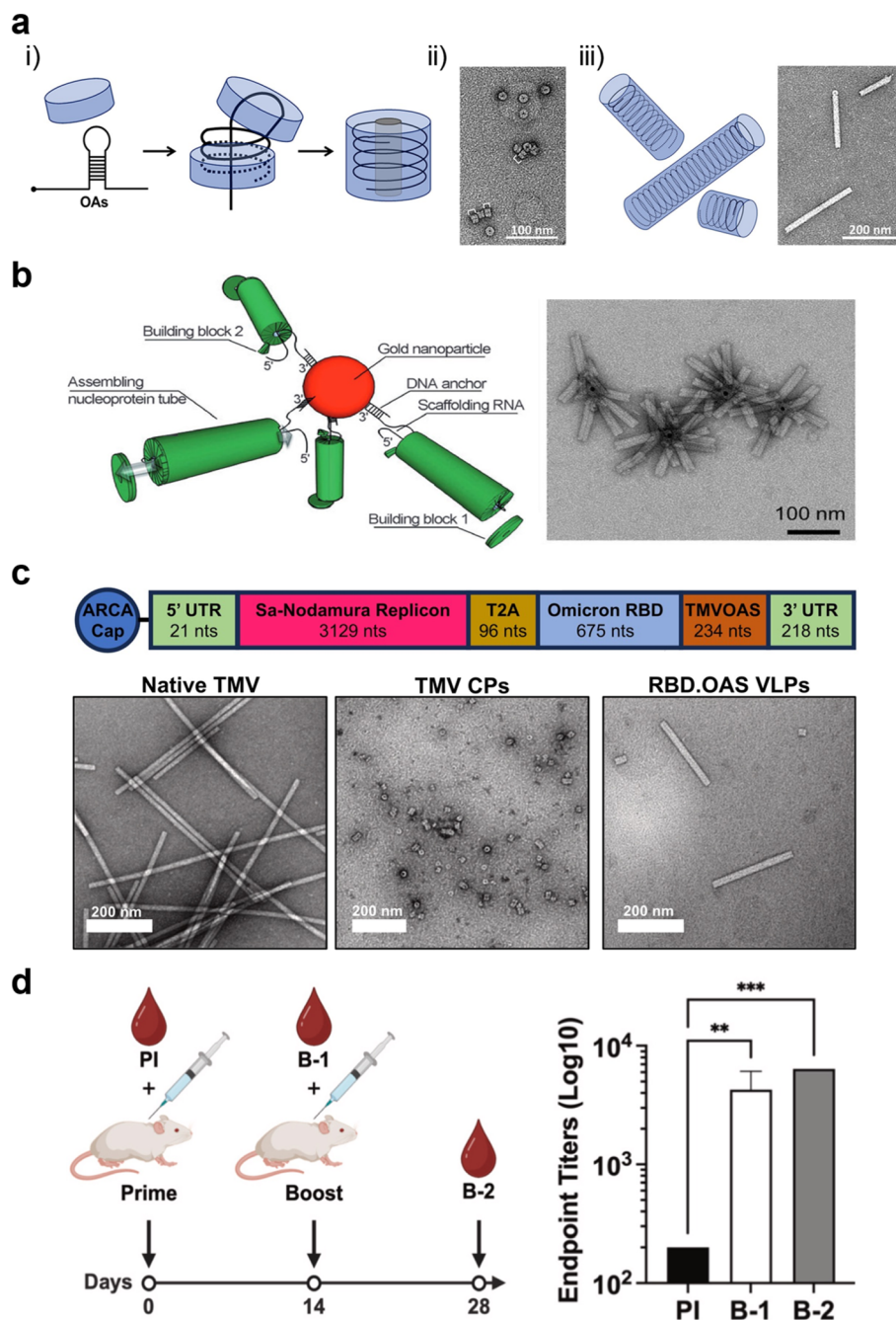


**Fig. 3** Self-assembly and application of TMV VLPs for nucleic acid therapeutics. (a) Production of TMV VLPs by assembly of TMV CPs. Origin of assembly sequence (OAS)-containing RNA-directed assembly of VLPs (i). TEM micrographs of short TMV VLPs (ii) and long TMV VLPs (iii). Reproduced from ref. 101 with permission from John Wiley and Sons, copyright 2019. (b) Schematic and TEM micrograph of star-like structure made of gold nanoparticle core and TMV VLP arms. Reproduced from ref. 106 with permission from John Wiley and Sons, copyright 2013. (c) Full mRNA construct encoding Nodamura RNA-dependent RNA polymerase and Omicron receptor-binding domain (RBD) with TMV OAS (top) and TEM micrographs of TMV, TMV CPs and reassembled TMV VLPs containing mRNA encoding RBD (RBD.OAS VLPs; bottom). (d) Immunization with TMV VLP carrying RBD-encoding mRNA (left) and endpoint antibody titers of anti-Omicron RBD elicited by VLP-mediated immunization (right). Reproduced from ref. 54 with permission from Elsevier, copyright 2025.

RNA-directed polymerization can generate programmable TMV-based VLPs.<sup>101</sup> TMV CPs can self-assemble into diverse structures, including star-like and boomerang forms *via* OAS-containing RNA-guided assembly (Fig. 3b).<sup>106,114</sup> Only ssRNA is encapsidated, so DNA-RNA hybrid structures can be used as stop signs to control the polymerization of TMV CPs.<sup>115</sup> CPs with

different functionalities can be mixed in a single TMV particle.<sup>116</sup> TMV-based VLPs can be modified by genetic and chemical engineering to facilitate applications in MRI imaging, vaccine development, and drug delivery.<sup>117–119</sup> Finally, the nucleoprotein components of TMV or its CPs can be heat-



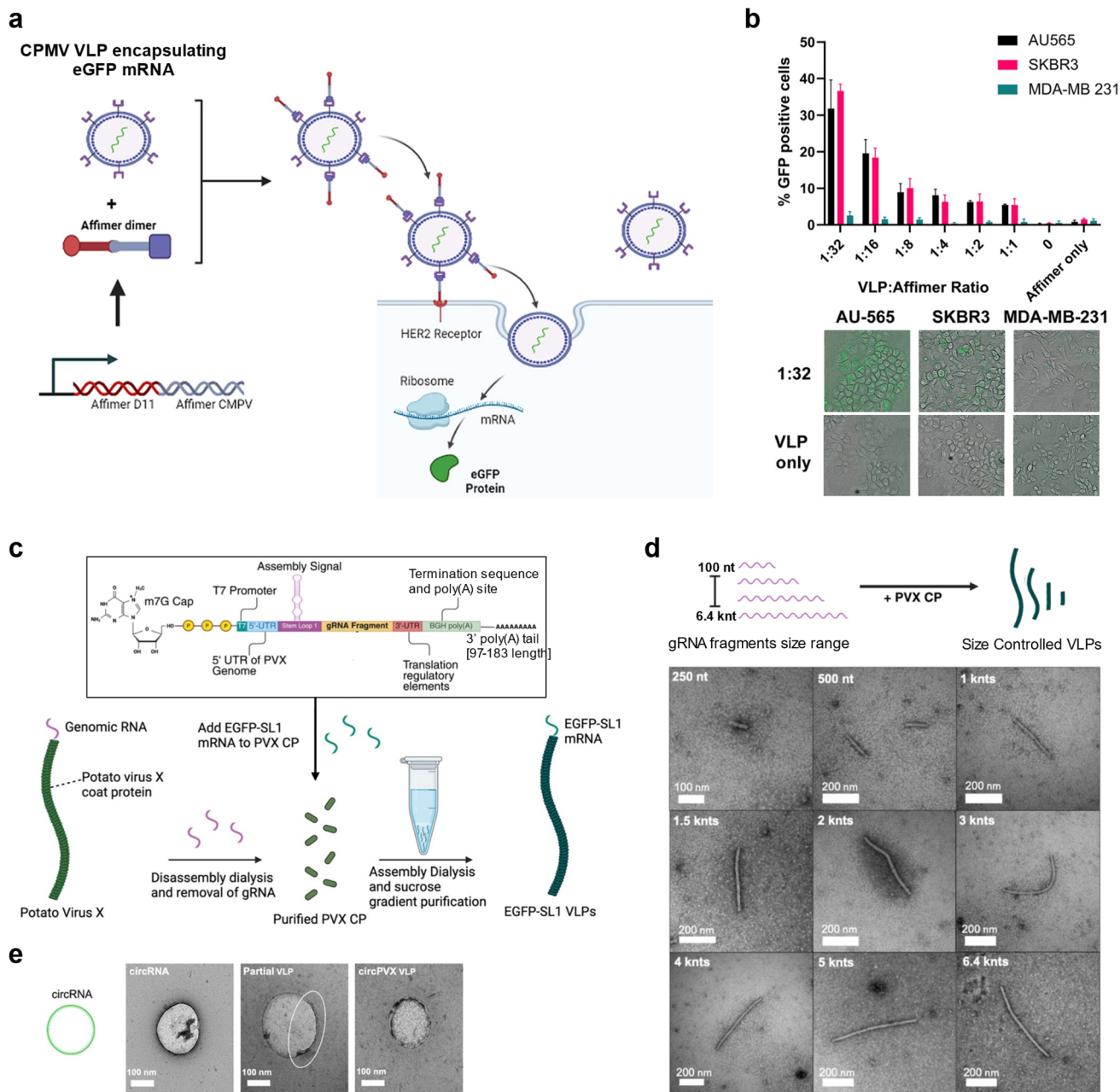


**Fig. 4** Applications of CPMV and PVX VLPs for the delivery of RNA therapeutics. (a) HER2-binding Affimer-mediated intracellular gene delivery and expression of CPMV VLPs carrying eGFP mRNA. (b) HER2-targeted delivery of CPMV VLPs to HER2<sup>+</sup> AU565 and SKBR3 cells using Affimers. VLP-to-Affimer ratio-dependent eGFP expression (top) and fluorescence images showing higher eGFP expression in HER2<sup>+</sup> cells compared with HER2<sup>-</sup> MDA-MB-231 cells (bottom). Reproduced from ref. 129 with permission from Elsevier, copyright 2024. (c) Full mRNA construct for PVX VLP assembly and production process of PVX VLP by assembly of PVX CPs with mRNA scaffold containing SL1 sequence. (d) Size controlled fabrication of VLPs depending on the length of RNA scaffolds and the TEM micrographs of resulting VLPs. (e) TEM micrographs of circular RNA and PVX VLPs containing circular RNAs. Reproduced from ref. 131 with permission from Springer Nature, copyright 2025. eGFP = enhanced green fluorescent protein, SL1 = stem loop 1, gRNA = genomic RNA, circRNA = circular RNA, circPVX = circular RNA-encapsulating PVX VLP.

annealed at spherical nanoparticles that can package small molecule drugs or nucleic acid therapeutics.<sup>120–123</sup>

### 3.3 The cowpea mosaic virus system

Cowpea mosaic virus (CPMV) is a member of the family *Comoviridae* and has a bipartite positive-sense ssRNA genome

comprising 6-kb RNA-1 and 3.5-kb RNA-2.<sup>124,125</sup> The CPMV particle is composed of 60 copies each of large (L) and small (S) CP subunits that assemble into a 30-nm icosahedral capsid.<sup>126</sup> Native CPMV can be produced *in planta* with a yield of 0.5–2 g kg<sup>-1</sup> of infected leaf tissue.<sup>127</sup> CPMV VLPs encapsulating heterologous mRNA can be generated *in planta* by infiltrating leaves with *Agrobacterium tumefaciens* carrying the pEAQ (“easy



and quick") transient expression vector, with a typical yield of  $\sim 1 \text{ g kg}^{-1}$  leaves.<sup>128,129</sup> A three-component system has been developed for *in planta* VLP assembly, comprising RNA-1, the CP precursor VP60, and a target gene inserted in the RNA-2 cassette, based on the finding that encapsidation is dependent on RNA replication.<sup>128,129</sup>

Using the pEAQ system,  $\sim 5\%$  of VLPs were shown to encapsulate *eGFP* mRNA (Fig. 4a).<sup>129</sup> By conjugation to a dimeric Affimer targeting human epidermal growth factor receptor 2 (HER2) and CPMV, the VLP achieved the HER2-specific internalization and expression of *eGFP* (Fig. 4b).<sup>129</sup> Notably, the three-component VLP production system allows CPMV VLPs to encapsulate ssRNAs ranging from 1.4 to 7.6 kb, exceeding the size of CPMV genomic RNA.<sup>130</sup> CPMV VLPs could be developed as vaccine candidates by encapsidating mRNAs that encode antigens such as the SARS-CoV-2 spike protein or the full-length glycoprotein of Ebolavirus.<sup>130</sup>

Besides its use as a gene delivery vehicle, CPMV has found application in cancer therapy: The immunomodulatory activity of CPMV facilitates cancer immunotherapy,<sup>132–134</sup> with potent efficacy demonstrated in mouse tumor models<sup>52,133–141</sup> and canine cancer patients.<sup>142–147</sup> Mechanistically, the nucleoprotein complex of CPMV acts on innate immune cells to modulate the tumor microenvironment (TME); the packaged RNA activates toll-like receptor (TLR)-7 and the capsid protein activates TLR-2 and -4. While the RNA is not expressed it plays a central role in the mechanism of action of CPMV as an immunotherapy candidate for cancer therapy. Intratumoral CPMV activates and recruits innate immune cells, thereby initiating a cascade of tumor killing mechanisms, resulting in the efficient presentation of tumor-associated and neoantigens, and the elicitation of adaptive anti-tumor immunity *via* tumor antigen-specific CD4<sup>+</sup> and CD8<sup>+</sup> effector and memory T cells.<sup>135,148</sup> Intratumoral CPMV thus induces an antitumor response against not only the treated tumor but also untreated distant tumors.<sup>149</sup>

### 3.4. Other plant viruses

Potato virus X (PVX) is a flexuous filamentous virus containing a 6.4-kb positive-sense ssRNA genome with a 5' cap and 3' polyadenylate tail.<sup>150</sup> The PVX particle contains 1300 25-kDa CP subunits that self-assemble into filamentous structure 515 nm in length and 13 nm in diameter with 8.9 CPs per helical turn.<sup>151</sup> RNA encapsulation requires a stem loop 1 (SL1) RNA sequence to bind CP and initiate VLP formation *in vitro*.<sup>152,153</sup> We recently developed PVX VLPs as an RNA delivery platform<sup>131</sup> and showed that PVX VLPs can encapsidate ssRNA molecules over a broad size range, including linear and circular RNA, as long as the SL1 sequence is present (Fig. 4c–e). The surface of PVX can be modified by incorporating His-tagged CPs, and the ability of PVX VLPs carrying the *eGFP* gene to express the corresponding protein highlights their versatility for the delivery of RNA therapeutics.

Physalis mottle virus (PhMV) is another positive-sense ssRNA virus with an icosahedral capsid  $\sim 30 \text{ nm}$  in diameter.<sup>154</sup> The PhMV particle comprises 180 identical CP units that display 720 surface lysine residues, enabling customization for applications

in drug delivery and imaging.<sup>155,156</sup> VLPs of PhMV are readily obtained through expression of the CP in *E. coli*.<sup>157</sup> PhMV VLPs have been developed as cancer vaccine candidates by incorporating CpG ODNs as an adjuvant to boost immune responses, while displaying the HER2-derived CH401 epitope.<sup>158</sup> CpG ODNs did not significantly enhance the immunogenicity of the particles but the study nevertheless demonstrated the potential of PhMV to encapsulate therapeutic DNA.

Brome mosaic virus (BMV), like CCMV, is a member of the family *Bromoviridae*.<sup>159</sup> It has a tripartite positive-sense ssRNA genome and forms icosahedral particles 28 nm in diameter composed of 180 copies of a 20-kDa CP.<sup>159,160</sup> Like CCMV, BMV can be disassembled into protein dimers and then reassembled as empty or cargo-packaged VLPs.<sup>86,161</sup> One study showed that BMV CPs can self-assemble with siRNA into icosahedral VLPs under the conditions used to prepare CCMV VLPs.<sup>86</sup> BMV can encapsulate  $\sim 66$  siRNA molecules per VLP, corresponding to the overall negative charge of the wild-type BMV.<sup>86</sup> BMV VLPs encapsulating anti-cancer siAkt1 delayed tumor growth with an efficacy comparable to CCMV VLPs without inducing immune responses, highlighting their potential as platforms for nucleic acid therapy.<sup>86</sup>

## 4. Bacteriophages as vehicles for nucleic acid delivery

### 4.1 The bacteriophage MS2 system

Bacteriophage MS2, a member of the family Leviviridae, contains a 3.57-kb positive-sense ssRNA genome encapsulated in a 27-nm icosahedral capsid composed of 180 identical CP subunits.<sup>162</sup> The assembly of the MS2 capsid *in vitro* and *in vivo* is initiated when a CP subunit binds to the *pac* site at the 5' end of the viral genome.<sup>163</sup> By including a *pac* site, MS2 VLPs can encapsulate heterologous ssRNA molecules.<sup>164,165</sup> The affinity between the *pac* site and MS2 CPs can be increased by replacing the uridine residue with cytidine at position  $-5$  in the *pac* site,<sup>166</sup> allowing the packaging of long heterologous RNAs up to 3000 nt length.<sup>167</sup> A second *pac* site increases CP binding affinity even further through cooperative binding.<sup>168</sup> The genetic or chemical modification of MS2 CPs allows protein and peptide display, making the VLPs versatile platforms for vaccine development and targeted drug delivery.<sup>169–171</sup>

MS2 VLPs encapsulating therapeutic mRNAs and vaccines can be produced in *E. coli* and yeast.<sup>163,165,172–175</sup> For example, MS2 CPs have been engineered to encapsidate a 1.5-kb ASO targeting the 5' region of the hepatitis C virus (HCV) genome.<sup>165</sup> Plasmid constructs encoding MS2 structural proteins and the HCV ASO plus *pac* site, respectively, were introduced into *E. coli* to produce the VLPs.<sup>165</sup> Chemical modification with the cell-penetrating TAT (transactivation of transcription) peptide activated human immunodeficiency virus 1 (HIV-1) and enhanced delivery to cancer cells, resulting in the inhibition of HCV translation in Huh-7 cells.<sup>165</sup> Similarly, MS2 CP was co-expressed with a heterologous mRNA in yeast to yield engineered MS2 VLPs encapsulating the mRNA cargo (Fig. 5a).<sup>175</sup> Adding more *pac* sites to the mRNA significantly enhanced the



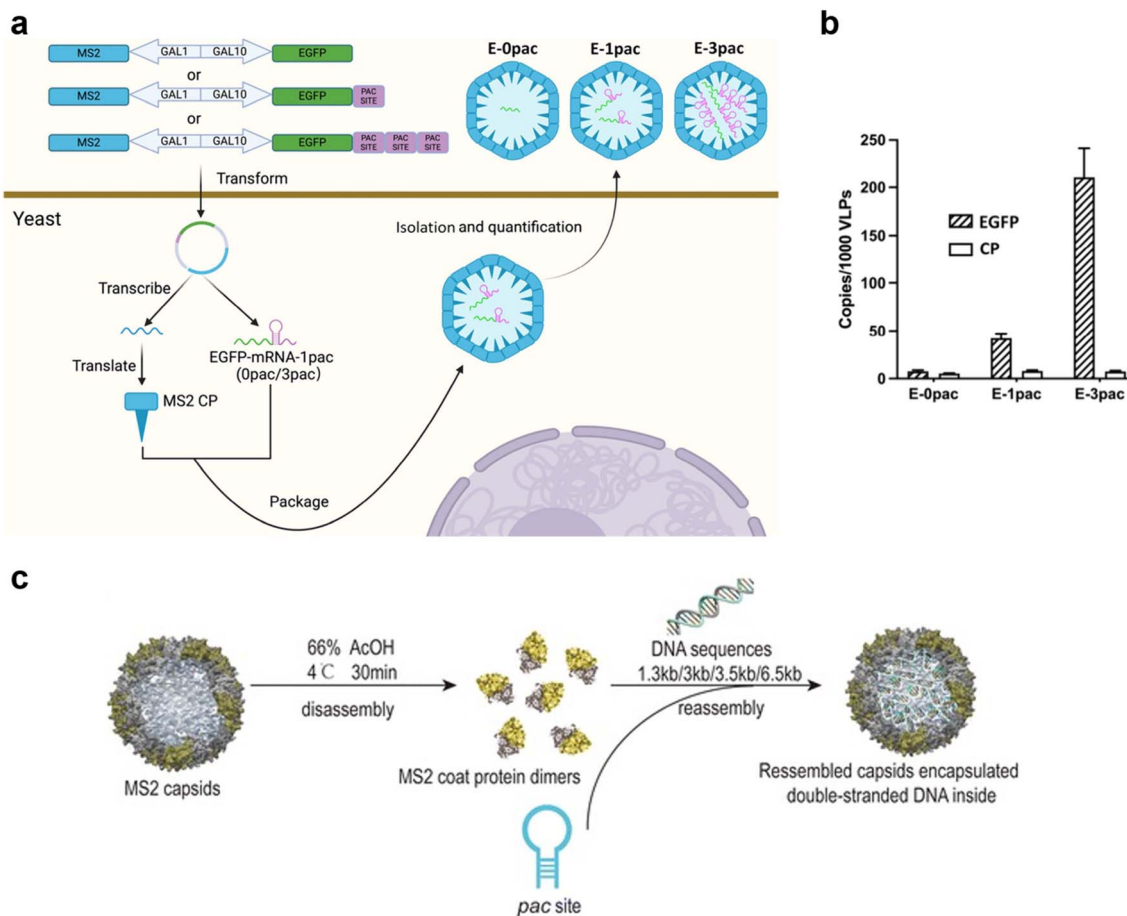


**Fig. 5** Application of MS2 VLPs for the delivery of nucleic acid therapeutics. (a) Production of MS2 VLPs encapsulating eGFP mRNA by the co-expression of MS2 CP and eGFP mRNA with different numbers of *pac* sites in yeast. (b) The number of mRNA copies encoding eGFP or CP encapsulated in 1000 VLPs depended on the number of *pac* sites. Reproduced from ref. 175 with permission from American Chemical Society, copyright 2025. (c) The fabrication of MS2 VLPs by reassembly of MS2 coat proteins with dsDNA conjugated with *pac* site. Reproduced from ref. 176 with permission from Springer Nature, copyright 2015.

selective packaging of the target mRNA while minimizing the incorporation of host or viral RNA (Fig. 5b).<sup>175</sup>

An early application of MS2 VLPs was the delivery of mRNA encoding human growth hormone (hGH) to CHO-K1 cells.<sup>173</sup> VLPs with heterologous mRNA could be prepared by self-assembly in the yeast *Saccharomyces cerevisiae* carrying two plasmid vectors for the MS2 CP and cargo mRNA.<sup>173</sup> This was extended to a VLP-based mRNA vaccine platform for HIV-1 by packaging mRNA encoding the HIV-1 Gag protein, which was achieved by *in situ* packaging in yeast.<sup>174</sup> The VLP-based mRNA vaccine induced Gag-specific antibody production *in vivo*.<sup>174</sup> MS2 VLPs have also been developed as prophylactic cancer vaccines.<sup>177</sup> An mRNA vaccine against prostate cancer was developed by transforming yeast with plasmids encoding MS2 CP and GM-CSF linked to the prostate-extensive antigen (PAP) and a C-variant *pac* site.<sup>177</sup> Systemic delivery of these MS2 VLPs elicited strong anti-tumor immunity characterized by delayed tumor progression and protection against tumor rechallenge.<sup>177</sup>

MS2 VLPs carrying miRNAs have been used for gene silencing.<sup>172</sup> In the initial report, a ~93-nt pre-miR146a was encapsulated during VLP synthesis in *E. coli*.<sup>172</sup> Chemical

conjugation with the cell-penetrating TAT peptide enhanced the delivery and expression of miR146a by up to 14-fold *in vitro* and 2-fold *in vivo*.<sup>172</sup> TAT-conjugated MS2 VLPs with pre-miR146a inhibited disease progression in lupus-prone mice and suppressed osteoclast differentiation, offering a new treatment for osteoporosis.<sup>178,179</sup> Similarly, MS2 VLPs displaying the epidermal growth factor receptor (EGFR) ligand GE11 achieved the targeted delivery of miRNAs to hepatocellular carcinoma cells (HCCs).<sup>180</sup> Co-packaging miR-122 with miR-21-sponge enabled the simultaneous delivery of both RNA molecules, resulting in the repression of HCCs.<sup>180</sup> Surface display has also been used to expose the TAT peptide, showing that the MS2-based RNA delivery platform can be functionalized by genetic and chemical modification.<sup>181</sup>

The MS2 capsid disassembles when exposed to acetic acid and reassembles into empty or packaged VLPs when the pH is neutral.<sup>182–184</sup> Thus packaging of cargoes through dis- and reassembly can be achieved: the linkage of anti-Bcl2 siRNA with a 5' *pac* site resulted in the formation of VLPs, and targeted delivery to HeLa cells was achieved by the display of human transferrin, resulting in Bcl2 knockdown and apoptosis



comparable to a commercial transfection reagent.<sup>183</sup> It was also shown that siRNAs are easily encapsulated during *in vitro* capsid assembly even in the absence of the *pac* site, resulting in more than 80 siRNA molecules encapsulated in a single VLP.<sup>184</sup>

Even ssDNA and dsDNA can be encapsulated in MS2 VLPs. For example, the 3' end of a 20-nt ODN targeting p120, an abundant nucleolar protein in leukemia cells, was attached to the TR region using a U4 linker.<sup>185</sup> The ODN was packaged into VLPs by *in vitro* assembly with MS2 CPs, enabling efficient delivery and demonstrating enhanced cytotoxicity in leukemia

HL-60 cells compared to naked ODN.<sup>185</sup> MS2 VLPs have been shown to encapsulate dsDNA in the size range 1.3–6.5 kbp without changes in capsid morphology or size despite being a native ssRNA virus (Fig. 5c).<sup>176,186</sup> Other non-RNA cargoes have been encapsulated in MS2 VLPs by chemical conjugation to the *pac* site, including quantum dots, drugs and toxins.<sup>184,187</sup> This greatly extends the applications of MS2 VLPs, which can be considered as multidrug delivery platforms.

Recent advances in the production and purification of MS2 VLPs include the use of sodium nitrate and pH to influence

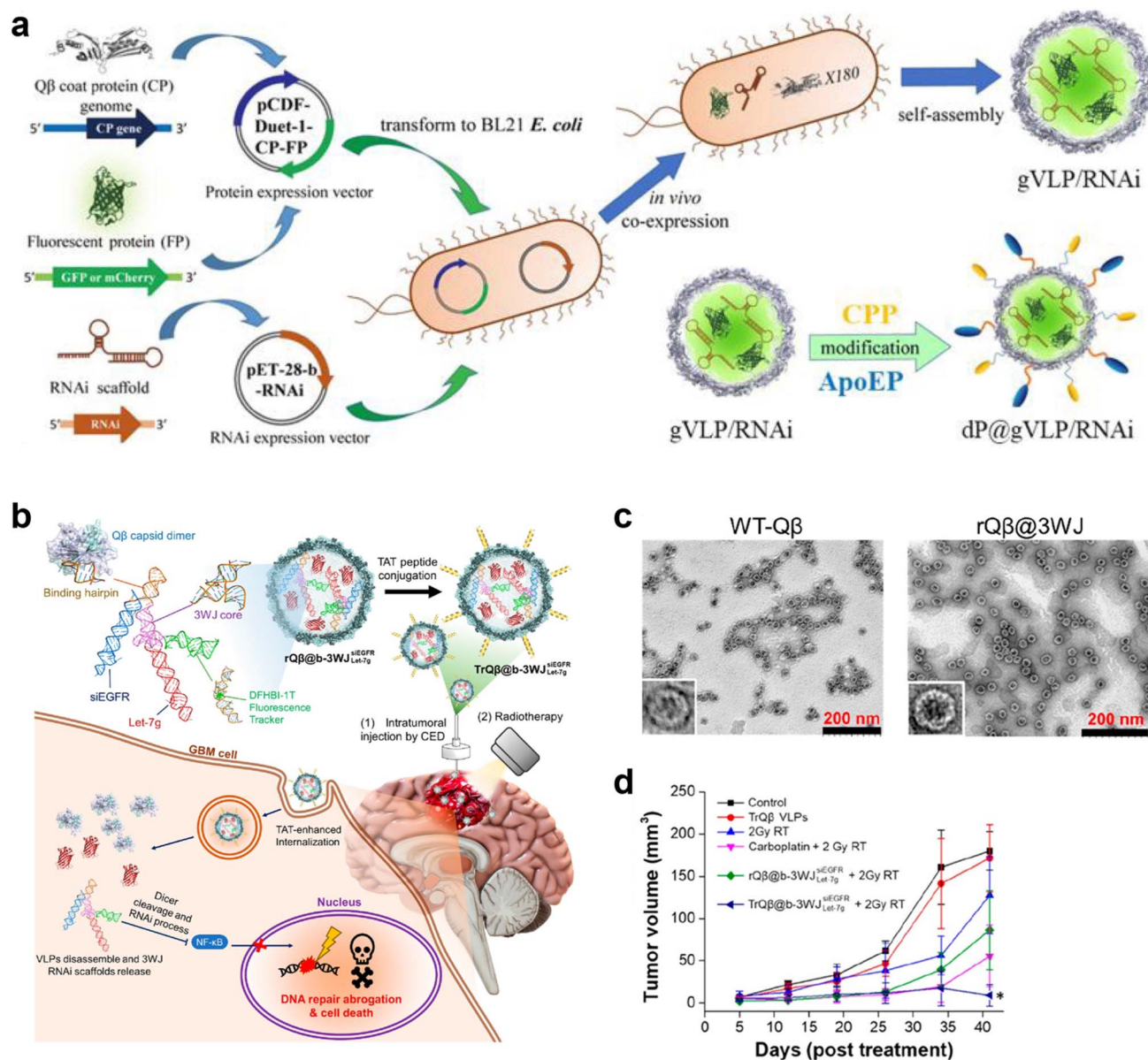


**Fig. 6** Applications of Qβ VLPs for the delivery of nucleic acid therapeutics. (a) Production of Qβ VLPs encapsulating RNAi molecules (gVLP/RNAi) in *E. coli* by co-expression of Qβ CP, RNAi scaffold, and fluorescent proteins followed by self-assembly and further surface modification with CPP and ApoEP (dP@gVLP/RNAi). Reproduced from ref. 209 with permission from Royal Society of Chemistry, copyright 2019. (b) Schematic illustration of Qβ VLP-mediated RNAi therapy for enhancing glioblastoma radiotherapy. Qβ VLPs encapsulate 3WJ RNA nanostructures carrying anti-EGFR siRNA and miRNA Let-7g, together with broccoli aptamer (rQβ@b-3WJ<sub>Let-7g</sub><sup>siEGFR</sup>). The Qβ VLP was further conjugated with TAT peptide (TrQβ@b-3WJ<sub>Let-7g</sub><sup>siEGFR</sup>). (c) TEM micrographs showing morphologies of wild-type Qβ (WT-Qβ) and Qβ VLP containing 3WJ (rQβ@3WJ). (d) Tumor growth after treatment. Reproduced from ref. 211 under the terms of the CC-BY-NC-ND 4.0 license (<https://creativecommons.org/licenses/by-nc-nd/4.0>). CED = convection-enhanced delivery, TrQβ VLPs = TAT-conjugated red-fluorescent Qβ VLPs.



particle size, uniformity and stability.<sup>188</sup> By varying these conditions, VLPs could be prepared with a size range of 27–30 nm and a minimum stability of 12 months at 4 °C.<sup>188</sup> The larger VLPs were able to carry more cargo as well as displaying more external peptides.<sup>189,190</sup> The insertion of a 13-amino-acid SpyTag peptide into an external loop of the MS2 CP increased the VLP diameter by ~4.4 nm and altered its geometry, favoring  $T = 4$  symmetry.<sup>189</sup> The larger particles were able to load ODNs and mRNAs with or without a *pac* site by diffusion through pores into the enlarged lumen, which remained fully protected from nucleases.<sup>190</sup> The exposed SpyTag binds strongly to the SpyCatcher ligand, enabling the display of complex proteins such as trimeric RBD.<sup>190</sup>

More recently, MS2 CPs have been used to encapsulate mRNA, guide RNA (gRNA) and ribonucleoprotein (RNP) molecules into synthetic VLPs derived from retroviruses<sup>191,192</sup> or lentiviruses.<sup>193–195</sup> For example, mRNA encoding Cas9 plus a *pac* site was co-expressed in host cells with a gRNA cassette in the integration-defective lentiviral vector (IDLV) and Gag proteins linked to the MS2 CP.<sup>193</sup> Given the high affinity between MS2 CP and the stem loop site, this resulted in the co-packaging of the *cas9* mRNA and gRNA cassette in all-in-one lentiviral particles.<sup>193</sup> The same group also developed gRNA-Cas9 RNP-encapsulating synthetic VLPs.<sup>194</sup> The gRNA (plus *pac* site) and Cas9 protein can assemble into RNPs that are co-packaged in the Gag-based VLPs, achieving efficient delivery and gene editing.<sup>194</sup> This highlights the adaptability and translational potential of MS2-based systems as next-generation platforms for nucleic acid therapeutics.

#### 4.2. The bacteriophage Q $\beta$ system

Bacteriophage Q $\beta$ , a member of the Leviviridae family like MS2, contains a ~4.2-kb positive-sense ssRNA genome encapsulated in a 28-nm icosahedral capsid composed of 180 identical CP subunits stabilized by disulfide bonds.<sup>196,197</sup> Q $\beta$  VLPs can be produced in *E. coli* by expressing the full-length Q $\beta$  CP, and the genomic RNA can be removed by RNase A treatment, allowing replacement with alternative cargo.<sup>198,199</sup> Q $\beta$  has shown particularly promising results for the delivery of CpG ODNs.<sup>198,200,201</sup> Cytos Biotechnology AG (Switzerland) reported that CpG ODNs can be encapsulated into Q $\beta$  VLPs by diffusion, achieving a loading capacity of up to ~85 DNA molecules per particle.<sup>200</sup> In mice treated with these VLPs, CD8<sup>+</sup> T cell activation was comparable to that induced by live vaccines, without the side effects associated with free CpG.<sup>200</sup> In a clinical trial, Q $\beta$  VLPs encapsulating CpG ODNs (vidutolimod) covalently coupled to a Melan-A antigen fragment for melanoma treatment induced both memory and effector CD8<sup>+</sup> T-cell responses in combination with imiquimod.<sup>202</sup> These VLPs also enhanced antitumor immune responses in combination with an anti-PD-1 antibody in metastatic and high-risk melanoma patients, and in mice with head and neck squamous cell carcinoma (HNSCC).<sup>203–205</sup> The opsonization of Q $\beta$  particles carrying CpG ODNs by anti-Q $\beta$  antibodies is needed to activate immune cells and induce pro-inflammatory immune responses.<sup>206</sup>

Q $\beta$  VLPs can be used as a vaccination platform without an adjuvant.<sup>207,208</sup> Q $\beta$  VLPs chemically conjugated to RBD or envelope protein domain III (EDIII) of Zika virus elicited neutralizing antigen-specific antibodies that conferred protective immunity.<sup>207,208</sup> Nonspecific bacterial RNA could be encapsulated as a TLR7/8 agonist, enabling the Q $\beta$  VLP to function as a self-adjuvanted vaccine together with antigen display.<sup>207,208</sup>

Besides its use as an adjuvant (making use of packaged CpG ODNs or RNA), the loading of Q $\beta$  VLPs with RNA during reassembly has been demonstrated for siRNAs targeting *c-MET* (encoding a receptor tyrosine kinase) linked to a CP-binding hairpin sequence at the 5' end.<sup>209</sup> The siRNAs were co-expressed with Q $\beta$  CP and GFP in *E. coli*, increasing the stability of the siRNA molecules, and were efficiently delivered to glioblastomas by displaying a CPP and blood-brain barrier-penetrating apolipoprotein E peptide on the VLP surface (Fig. 6a).<sup>209</sup> Disassembled Q $\beta$  CPs have also been reassembled with anti-*luc* siRNA, resulting in successful cytosolic delivery and knockdown (targeting mitochondria by conjugating a lipophilic triphenylphosphonium cation).<sup>210</sup> Q $\beta$  VLPs have also been engineered to encapsulate therapeutic RNAs using the  $\phi$ 29 three-way junction (3WJ) nanostructure, enabling the co-delivery of functional RNA modules such as siRNA, miRNA and aptamers, which synergistically enhanced therapeutic efficacy (Fig. 6b and c).<sup>211</sup> Notably, Q $\beta$  VLPs achieved potent therapeutic efficacy (>70% tumor growth inhibition) and significantly prolonged survival in glioblastoma-bearing mice while minimizing systemic toxicity by favoring localized convection-enhanced delivery (Fig. 6d).<sup>211</sup> These findings highlight the versatility of Q $\beta$  VLPs as a multifunctional platform for vaccine development and nucleic acid delivery.

#### 4.3. The bacteriophage M13 system

M13 is a filamentous bacteriophage of the family Inoviridae with a 6407-bp ssDNA genome packaged into a capsid 880 nm in length with a diameter of 6.6 nm.<sup>212</sup> The M13 capsid is mainly composed of the major coat protein (pVIII), which accounts for ~98% of the structure, but also contains four minor proteins (pIII, pVI, pVII and pIX) at the termini of the filament.<sup>213</sup> The genetic amenability of M13 has led to its widespread use as a phage display library for peptides and proteins, enabling the discovery of target-specific ligands for therapeutic and diagnostic applications.<sup>41,214</sup>

The ability of M13 to encapsulate DNA also makes it suitable for gene delivery to mammalian cells, which was first demonstrated using phagemid vectors (plasmids containing an M13/f1 origin of replication) and helper phage.<sup>215</sup> These M13 VLPs carried phagemids containing *GFP* or *lacZ* genes under the control of a cytomegalovirus (CMV) promoter for expression in mammalian cells, an M13/f1 origin for viral replication and packaging, and a plasmid origin for replication in *E. coli*.<sup>215</sup> The surface of the M13-like particles was modified by biotin-avidin conjugation to display fibroblast growth factor 2 (FGF2) to enable the FGF2 receptor-specific transduction.<sup>215</sup> Similarly, genetic modification of the M13 CP to display antibodies achieved targeted DNA delivery.<sup>216,217</sup> Decoration with a HER2-



specific antibody fused to pIII promoted the internalization of M13 VLPs by endocytosis, followed by robust gene expression.<sup>216</sup>

To overcome safety concerns reflecting the presence of bacterial sequences in the phagemid vector backbone,<sup>218,219</sup> unnecessary bacterial elements have been removed.<sup>220–223</sup> For example, the phagemid was miniaturized by splitting the  $f_1$  origin with the transgene cassette, resulting in a so-called miniphagemid.<sup>220</sup> During helper phage-mediated replication, M13 CPs could selectively replicate and package only the *ori*-flanked expression cassette, excluding bacterial backbone sequences without compromising rescue efficiency.<sup>220</sup> The miniphagemid-based M13 particles enabled targeted gene delivery and expression by displaying EGF to facilitate receptor-mediated internalization.<sup>221</sup>

The length of recombinant M13 VLPs is dependent on the size of the packaged cargo, and transduction efficiency is inversely correlated with length.<sup>222,223</sup> A minimal M13 vector (TransPhage) carrying a 2384-nt transgene encoding membrane-bound Fc inhibited tumor growth in a xenograft model by triggering CD16<sup>+</sup> natural killer (NK) cells *via* a mechanism resembling antibody-dependent cell-mediated cytotoxicity (ADCC).<sup>222</sup> Key factors that increased transduction efficiency included upregulated *PrimPol* and downregulated *DMBT1* gene expression, achieving a remarkable ~95% transduction efficiency with the minimal vector.<sup>222</sup> Further reduction to 285 nt enabled the production of VLPs with precisely controlled lengths of 50 nm.<sup>223</sup> By fusing pIII to chlorotoxin (CTX), a scorpion venom peptide that specifically targets gliomas, the miniaturized CTX-VLP penetrated deeply into brain tumors and accumulated there.<sup>223</sup>

Despite the advances discussed above, M13-mediated gene delivery is hindered by inherently low transduction efficiencies in mammalian cells. A hybrid system combining AAV and phage (AAVP) has been developed by inserting the AAV inverted terminal repeats (ITRs) and a transgene cassette to the M13

genome to facilitate genomic integration.<sup>224–226</sup> A chimeric AAVP carrying an ITR-GFP transgene cassette induced stronger GFP expression in HEK 293 cells by targeting  $\alpha v$  integrin *via* an RGD-4C peptide displayed on pIII.<sup>224</sup> Intravenous administration of AAVPs carrying the herpes simplex virus (HSV) thymidine kinase (tk) gene, which acts as a suicide gene when combined with ganciclovir, resulted in targeted delivery and the suppression of tumor growth.<sup>224,227</sup> The same approach was used to deliver the tumor necrosis factor gene (*TNF $\alpha$* ) to human glioblastoma cells, again by targeting integrin  $\alpha v$ , inducing apoptosis and tumor reduction.<sup>227</sup> The recruitment of streptavidin-binding peptides to pVIII can generate multifunctional AAVPs, such as the addition of pH-sensitive fusogenic H5WYG peptides to promote endosomal escape and enhance gene delivery *in vitro* and *in vivo*.<sup>226</sup>

The AAVP system has been optimized in terms of vector size, AAVP length and transduction efficiency to facilitate clinical applications by minimizing the structural genes and utilizing helper phages (Fig. 7a and b).<sup>227–230</sup> The resulting transmorphic phage/AAV particles (TPAs) are 50% shorter than AAVP,<sup>228,229</sup> which enabled faster delivery and higher transduction and diffusion efficiencies in an *in vitro* glioblastoma multiforme spheroid model compared to AAVP.<sup>228</sup> The systemic delivery of TPA displaying RGD-4C and carrying an *IL-12* transgene induced tumor-localized IL-12 expression to suppress tumor growth and increase survival (Fig. 7c).<sup>228</sup> Similarly, a TPA carrying the *TRAIL* gene (encoding TNF-related apoptosis-inducing ligand) was able to selectively transduce HCC cells and induce apoptosis.<sup>230</sup>

The M13 genome contains unmethylated CpG motifs that can induce an innate immune response *via* TLR9 signaling, supporting its potential as a vaccine platform.<sup>231–233</sup> The immunogenicity of M13 can be enhanced by incorporating more CpG sequences, particularly CpG hexamers.<sup>232</sup> These reprogrammed phages (RPs) were used as a vaccine against MC-

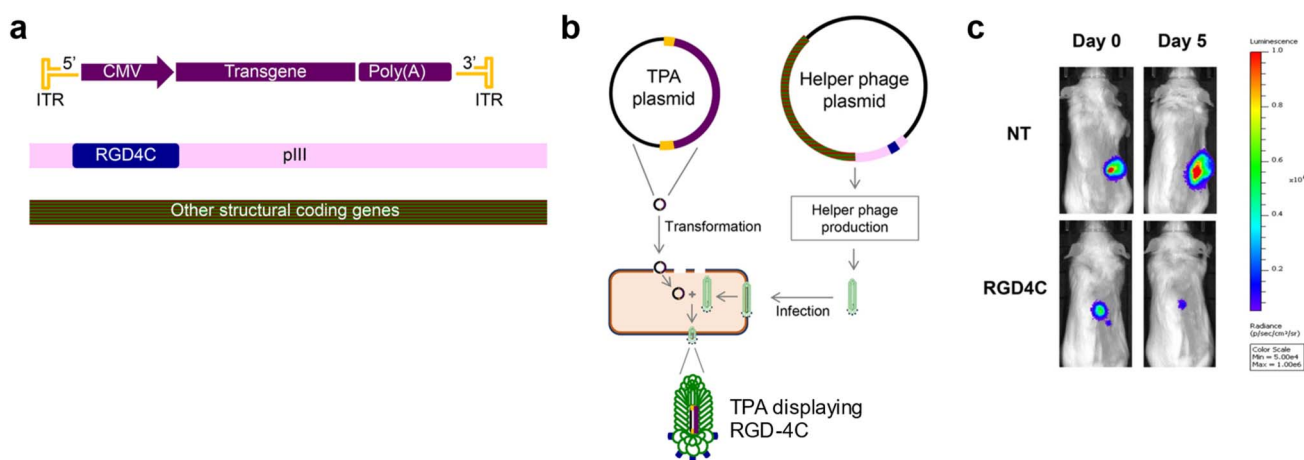


Fig. 7 Application of M13 VLPs for gene delivery. (a) Constructs for transmorphic phage/AAV particles (TPA) production: constructs encoding transgene cassette flanked by inverted terminal repeats ITRs (top), RGD4C-conjugated pIII (middle) and structural coding genes for helper phages (bottom). (b) Production of transgene-carrying TPA displaying RGD-4C at pIII using TPA plasmid with ITR-transgene cassette and helper phage expressing RGD-4C on coat protein pIII in *E. coli*. (c) Bioluminescence imaging of luciferase-expressing CT26 tumors on days 0 and 5 post-treatment showing *in vivo* anti-tumor efficacy of IL-12-encoding TPA (NT) and RGD-4C-displaying TPA (RGD4C). Reproduced from ref. 228 with permission from Springer Nature, copyright 2022. CMV = cytomegalovirus promoter region.



38 colon cancer by encoding neoantigen ADPGK fused to pVIII. The RP phages accumulated in and activated antigen-presenting cells (APCs), followed by the activation of ADPGK-specific CD8<sup>+</sup> T cells, showing potential for the development of personalized cancer vaccines.<sup>232</sup>

The large surface area of M13 can incorporate other functional biomaterials or nanoparticles for further customization. For example, the negatively charged M13 capsid has been complexed with a positively charged polymer to enhance delivery.<sup>234</sup> A positively charged polymer coating was shown to increase the accessibility of M13 displaying RGD peptides, boosting the expression of luciferase (Luc) in cancer cells by ~10-fold without disrupting  $\alpha$ v integrin-specific delivery.<sup>234</sup> The decoration of AAVPs carrying a hemagglutinin (HA) transgene with MnO<sub>2</sub> nanoparticles facilitated the development of an influenza vaccine by the co-delivery of antigen and adjuvant in a single particle.<sup>235</sup>

Finally, M13 has also been used for gene silencing and genome editing in bacteria.<sup>236,237</sup> Phagemids encoding 24-nt RNA ASOs targeting ribosomal protein genes needed for bacterial growth were encapsulated in M13 particles and were shown to reduce the viability of multidrug-resistant bacteria, demonstrating their potential as antibacterial therapeutics.<sup>236</sup> Moreover, phagemids carrying *cas9* and gRNA genes have been packaged in M13 particles to enable selective genomic deletions in target species of the gut microbiome *via* oral gavage in mice.<sup>237</sup> These findings highlight the versatility and broad applicability of M13 as a gene therapy platform, also extending its applications to antibacterial therapeutics.

#### 4.4. The bacteriophage T4 system

Bacteriophage T4 is a classic coliphage of the family *Straboviridae*, containing a ~170-kbp dsDNA genome packaged in a large

prolate capsid (115 nm x 85 nm) appended to a ~100-nm contractile tail with fibers for host recognition.<sup>238,239</sup> The capsid features more than 40 structural proteins, including two accessory proteins on the surface: highly immunogenic outer capsid protein (Hoc) and small outer capsid protein (Soc).<sup>238,239</sup> It rapidly packages its genomic DNA through the portal vertex of the empty prohead *via* ATP hydrolysis-driven translocation mediated by the ATPase of gp17.<sup>240</sup>

T4 particles have been engineered for the simultaneous delivery of genes and proteins as an advanced vaccine platform.<sup>65,241</sup> The neckless and empty T4 heads produced in *E. coli* can rapidly package single or multiple dsDNA molecules ranging from 2.3 to 170 kbp in the presence of gp17 ATPase and ATP (Fig. 8a).<sup>65,242</sup> A single dose of T4 particles decorated with the DEC205 antibody fused to Hoc and the F1-V antigen fused to Soc elicited strong and sustained T cell stimulation.<sup>65</sup> This platform has also been used to develop a universal SARS-CoV-2 vaccine carrying multiple antigens on its surface and within the capsid structure, including RBD, nucleoprotein, and the 6.5-kb spike protein gene.<sup>241</sup> This vaccine candidate elicited robust, antigen-specific and balanced Th1/Th2 immune responses, providing complete protection against viral challenge even without adjuvant.<sup>241</sup>

Despite its natural specificity for bacteria, T4 has been engineered for efficient gene delivery to mammalian cells. For example, it has been decorated with 25-nm AAV particles using avidin–biotin conjugation to Soc.<sup>243</sup> These AAV-tethering T4 particles were able to encapsulate nine copies of the 6.2-kbp *luc* gene flanked by AAV ITRs, enabling the co-delivery and co-expression of genes and proteins carried by T4 and AAV, enhancing T4 transduction into mammalian cells by ~40 000-fold.<sup>243</sup> Moreover, cationic lipid coating also enhanced cargo gene expression by ~1 000 000-fold compared to uncoated T4 phages (Fig. 8a).<sup>242</sup> Notably, 2.5 molecules of a ~20-kbp

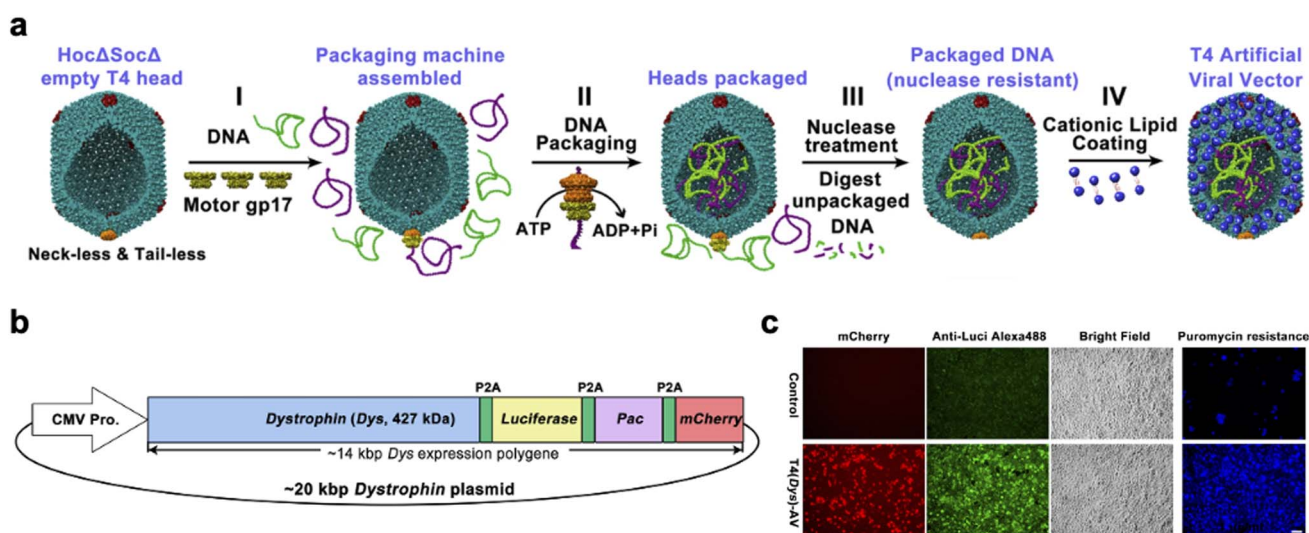


Fig. 8 Application of T4 AAVP VLPs for gene delivery. (a) Packaging of DNA into neck-less and tail-less T4 head by gp17 ATPase followed by cationic lipid coating. (b) DNA construct encoding 20-kbp polygene of 427-kDa human dystrophin protein and reporter proteins. (c) Reporter gene expression in HEK293T cells by T4 AAVP encapsulating dystrophin and reporter proteins. Scale bar: 50  $\mu$ m. Reproduced from ref. 242 with permission from Springer Nature, copyright 2023.



polygene encoding the 427-kDa human dystrophin protein and a reporter protein was encapsulated in T4 heads, even though this is too large to be encapsulated in AAV (Fig. 8b and c).<sup>242</sup> Cationic lipid coated T4 particles also allow the delivery of RNP complexes to human cells, including a Soc-fused Cas9 protein with gRNA, mRNA or siRNA, which can be mixed and matched for combinatorial and multifunctional use.<sup>242</sup>

T4 has also been used to deliver therapeutic genes to bacteria in the gut microbiome, enabling the production of target proteins *in situ*.<sup>244</sup> Initially, the super-fold GFP gene (*sfGFP*) was placed under the control of early T4 promoters that are highly active during viral infection, resulting in significant sfGFP production *in vitro* and *in vivo*.<sup>244</sup> The oral delivery of T4 encapsulating the gene encoding satiety-inducing endogenous chaperone protein (ClpB), a conformational mimetic of the human appetite-regulating hormone  $\alpha$ -MSH, resulted in strong gene expression in the gut, leading to reduced weight gain in a mouse diet-induced obesity model.<sup>244</sup> T4 has also been used to deliver plasmid DNA based on electrostatic interactions with poly-L-lysine-modified T4 capsids containing multiple drugs for enhanced chemodynamic therapy.<sup>245</sup> In this system, the engineered T4 particles were loaded with lactate oxidase fused to Soc and dextran iron-based Fenton catalysts together with hypoxia-responsive DNA encoding Keap1, enabling the modulation of the TME.<sup>245</sup> These studies demonstrate that T4 can be used to reprogram mammalian cells or bacteria by controlling gene expression.

#### 4.5. The bacteriophage $\lambda$ system

Bacteriophage  $\lambda$  has a similar morphology to T4, with a 48.5-kbp dsDNA genome packaged in a 60-nm icosahedral capsid appended to a 150-nm tail structure for host cell recognition and viral genome delivery.<sup>246</sup> Given its natural ability to infect *E. coli*,  $\lambda$  has been widely used for genome editing in the gut microbiome.<sup>247–249</sup> However, its stability and ability to package substantial amounts of heterologous DNA provide an ideal platform for eukaryotic gene and vaccine delivery.<sup>250,251</sup>

The delivery of genes to mammalian cells by bacteriophage  $\lambda$  was demonstrated first in 1971 by expressing a galactose transferase transgene in human fibroblasts.<sup>252</sup> With advances in  $\lambda$  engineering, cell targeting has been improved by decorating the V protein with RGD peptides or the D protein with the integrin-binding penton base of adenovirus.<sup>253–255</sup> Later, bacteriophage  $\lambda$  was used to deliver antigen genes under the control of the CMV promoter for immunization in mice and rabbits.<sup>256–258</sup> The expression of eGFP driven by the CMV promoter elicited a stronger antibody response than naked DNA even when the number of DNA copies was 200-fold lower, indicating the efficient targeting and activation of APCs.<sup>256</sup> Bacteriophage  $\lambda$  has been explored as a vaccine for hepatitis B, showing a high antigen-specific antibody production in rabbits following vaccination with particles carrying the hepatitis B surface antigen.<sup>257,258</sup>

Similarly, bacteriophage  $\lambda$  has been developed as an HPV vaccine to prevent cervical cancer. The HPV-16 E7 oncogene was cloned in the vector  $\lambda$ ZAP-CMV and packaged into VLPs.<sup>259</sup> Injecting the VLPs induced an anti-tumor response, but wild-

type bacteriophage  $\lambda$  also showed immunostimulatory effects.<sup>259</sup> VLPs containing a  $\lambda$ ZAP-CMV-apoptin expression cassette induced apoptosis in breast cancer cells but not in normal cells, even without tumor-targeting ligands.<sup>260</sup>

#### 4.6. Other bacteriophages

Several other bacteriophages, such as Tan2, have been used to deliver CRISPR/Cas9 components into bacteria for genome editing by encapsulating phagemid vectors and using helper phages.<sup>261–263</sup> Focusing on mammalian cells, PP7 (carrying an ssRNA genome) has been shown to package and protect heterologous RNA, allowing the development of VLPs displaying the TAT peptide and encapsulating pre-miR-23b linked to a *pac* site.<sup>264</sup> The pre-miR-23b was delivered to and processed in human cells, successfully inhibiting genes involved in cell mobility.<sup>264</sup> Bacteriophage P22 has been used to encapsulate gRNA-Cas9 RNPs by fusing Cas9 to a P22 scaffold protein.<sup>265</sup> These studies highlight the vast and still-expanding potential of bacteriophages as customizable and multifunctional delivery vehicles for nucleic acid therapeutics.

## 5. Safety and immunogenicity of plant viruses and bacteriophages

Although plant viruses and bacteriophages do not infect mammalian cells, successful clinical translation requires the assessment of toxicity and immunogenicity.<sup>266</sup> The latter is a double-edged sword because it enhances the efficacy of vaccines but can reduce the efficacy of therapeutics.<sup>267,268</sup>

Plant viruses and related VLPs have shown favorable safety profiles in multiple studies.<sup>39,269,270</sup> For example, CPMV particles were cleared from plasma within 20 min after a single injection and no toxicity was observed even at doses up to 100 mg kg<sup>-1</sup>.<sup>271,272</sup> Similar, PVX showed no evidence of inducing hemolysis, teratogenicity or lethal effects in early embryo assays, supporting the biocompatibility of plant viruses as nanocarriers.<sup>273</sup> Even after repetitive injections, plant viruses are well tolerated.<sup>46,139,274</sup>

Unmodified plant viruses are known to be immunogenic,<sup>111,134,275</sup> and this may be exploited therapeutically in vaccine and immunotherapy development. As discussed above, CPMV has a potent immunostimulatory effect that has been exploited in the context of intratumoral immunotherapy.<sup>133,134</sup> It has also been shown that TMV can induce the polarization of macrophages to an M1 phenotype by activating TLR4 signaling, as well as stimulating dendritic cells and T cell responses.<sup>111,112</sup>

However, the immunogenicity may be a hurdle for systemic application of plant viral gene delivery vectors, and more research is required to delineate the best application areas.

Like other nanoparticles, VLPs are cleared by immune cells and organs of the reticuloendothelial system (RES). Non-specific scavenging by macrophages, induced by the protein corona, can be reduced significantly by surface coating with stealth molecules such as polymers and serum albumin.<sup>57,276–278</sup> These coatings also shield the vectors from anti-carrier antibody recognition. Antibodies against the VLPs may be elicited during



treatment – but there is also prevalence of anti-plant viral antibodies, likely due to exposure through the food chain. In a test of serum samples from 50 de-identified patients, 52% were positive for CPMV, 92% for TMV, 18% for PVX, and none for CCMV.

When the target are immune cells, *i.e.* for intratumoral immunotherapy, pre-existing anti-CPMV antibodies are not neutralizing and can even enhance therapeutic efficacy *via* opsonization.<sup>139</sup> However, if the target are non-immune cells, careful testing and engineering will be needed to shield the VLPs from opsonization and premature immune cell clearance.<sup>279</sup>

Clinical trials have demonstrated the safety of bacteriophages, with most patients showing no adverse effects.<sup>280</sup> Although bacteriophages do not infect mammalian cells, they can interact with them, adhere to the surface, enter and accumulate within them.<sup>175,281,282</sup> Bacteriophages also induce immune responses based on their capsid, viral genome and/or host bacterial components.<sup>207,208,283</sup> More than 80% of human serum samples contain antibodies against the T4 major capsid protein and 60% contain antibodies against Q $\beta$ .<sup>139,284</sup> The bacterial RNA loaded into VLPs during assembly triggers TLR7 and TLR8 signaling.<sup>207,208</sup> Bacteriophage DNA has been detected in the blood of a chicken model more than 5 weeks after administration by oral gavage, but did not induce a strong immune response.<sup>283</sup> In contrast, unmethylated CpG motifs in bacteriophage M13 DNA induced the production of IgG, pro-inflammatory cytokines, and interferons.<sup>231,285,286</sup> Similarly, dsRNA isolated from MS2-infected bacteria elicited interferon production.<sup>287</sup> Moreover, high titers of antibodies against bacteriophage  $\lambda$  were detected during the development of a specific peptide-targeting vaccine.<sup>256–258</sup> These immunostimulatory effects can improve vaccine efficacy but could be reduced for therapeutic nucleic acid delivery by removing vector backbone sequences.<sup>220</sup> Increasing the number of *pac* sites in cargo RNA molecules enhances encapsulation while reducing the packaging of host RNA.<sup>222</sup> Low-immunogenicity bacteriophages could be selected for therapeutic nucleic acid delivery in the future.<sup>288</sup>

Plant viruses and bacteriophages (and corresponding VLPs) have shown favorable safety profiles and controllable immunogenicity in various preclinical models, with rapid plasma clearance and no systemic toxicity even at high doses. Their inability to replicate and broad biocompatibility support their translational potential. These findings suggest that plant viruses, bacteriophages and their VLPs are safe and adaptable vehicles for nucleic acid delivery. Their future clinical translation will depend on the development of application-specific design strategies to maintain or enhance immunogenicity for vaccine platforms while suppressing it for therapeutic gene delivery, achieving an optimal balance between safety, efficacy and immunomodulation.

## 6. Conclusions and future perspectives

Nucleic acid therapy has moved from concept to clinical reality, but progress has been hindered by inefficient delivery

platforms.<sup>2</sup> This review has considered plant viruses, bacteriophages and their VLPs as emerging platforms that overcome the drawbacks of both mammalian viruses and synthetic carriers: they are intrinsically unable to infect or replicate in mammalian cells, reducing risks of insertional mutagenesis;<sup>39</sup> they possess genetically and chemically modifiable capsids with well-defined geometries, achieving precise modular surface functionalization and multivalent display;<sup>44,289</sup> and they enable scalable manufacturing in plants, bacteria or yeast.<sup>241</sup> As such, they are versatile platforms for the delivery of siRNA, miRNA, mRNA, saRNA and DNA.

Despite this promise, several challenges must be overcome before broad clinical deployment becomes possible. Most plant viruses and bacteriophages lack tropism for mammalian cells and tissues, and thus require rationally designed mechanisms for internalization and cargo release.<sup>226,243</sup> Moreover, despite favorable safety and clearance profiles *in vivo*, the immunogenicity of plant viruses and bacteriophages must be controlled for applications such as immunotherapy and gene silencing. Recent strategies to address this include stealthing *via* surface coating with polymers or serum albumin, and genome miniaturization.<sup>57,220,276–278</sup> The dosage, pharmacokinetics, biodistribution, administration route, and breadth of immune responses of final formulations must be understood in detail to meet regulatory requirements.

The use of VLPs must be expanded to realize their full potential as nucleic acid therapeutics. Thus far, the delivery of genome editing components has relied mainly on mammalian viruses<sup>290–292</sup> or synthetic vectors.<sup>293–295</sup> Mammalian VLPs have been shown to efficiently package and deliver Cas9 RNPs, base editors, and prime editors *in vivo*, achieving high-efficiency genome editing.<sup>296–298</sup> These studies also introduced a directed evolution approach to mutate and select optimized VLP variants, thus improving yields and transduction efficiency.<sup>298</sup> Mammalian VLP platforms therefore represent a major advance toward genome-free delivery systems suitable for the clinic and provide a blueprint for the future engineering of non-mammalian VLPs.

Synthetic VLPs derived from retroviruses and lentiviruses have been used to encapsulate gRNA and Cas9 mRNA linked to a *pac* site and MS2 CP-linked structural proteins.<sup>192,193</sup> Cas9 RNPs have also been used as a universal drug-catching linker on the head of bacteriophage T4.<sup>242</sup> Bacteriophage M13 has been shown to deliver genome editing components to bacteria but not yet to mammalian cells.<sup>236</sup> Given the remarkable diversity of bacteriophages and plant viruses, these systems hold great promise as versatile carriers for a wide range of nucleic acid cargoes.

Non-mammalian viruses as delivery systems remain largely preclinical but there is steady progress in several therapeutic areas.<sup>299</sup> CPMV nanoparticles have shown preclinical safety and efficacy in animal models, including canine cancer patients, demonstrating potent immune activation and tumor regression.<sup>142–147</sup> A VLP based on papaya mosaic virus was recently tested in a phase I clinical trial as a TLR7 adjuvant for an inactivated trivalent influenza vaccine.<sup>300</sup> Bacteriophage Q $\beta$  VLPs encapsulating CpG ODNs have shown potent antitumor



efficacy in clinical trials, particularly when combined with monoclonal antibody therapy or TLR7 agonists.<sup>202–204</sup>

Looking forward, we anticipate that the convergence of structural virology, synthetic biology, nucleic acid nanotechnology, and computational design will enable the rational design of a new generation of non-mammalian viral carriers incorporating targeting ligands and endosome-escape peptides, allowing the co-delivery of nucleic acids and proteins. Importantly, molecular farming in plants and high-titer bacterial fermentation offer practical manufacturing routes that are modular, inexpensive, and globally scalable. Plant viruses, bacteriophages and their VLPs thus represent a rapidly maturing platform with the potential to reshape nucleic acid drug delivery, paving the way toward safe, tunable, and clinically adaptable nucleic acid delivery vehicles.

## Author contributions

DK: visualization, investigation, writing – original draft; BD: investigation, writing – original draft; MV: visualization, investigation; GG: investigation; NFS: conceptualization, supervision, writing – review & editing.

## Conflicts of interest

Dr Steinmetz is a co-founder of, has equity in, and has a financial interest in Mosaic ImmunoEngineering Inc. Dr Steinmetz is a co-founder of, and serves as manager of Pokometz Scientific LLC, under which she is a paid consultant to Ring Therapeutics, Inc. Dr Steinmetz is a co-founder and CEO of, has equity in, and has a financial interest in PlantiosX Inc. The other authors declare no potential conflicts of interest.

## Data availability

No primary research results, software or code have been included and no new data were generated or analysed as part of this review.

## Acknowledgements

This work was funded in part by the NIH R01-CA224605 grant and an Accelerating Innovations to Market (AIM) grant through UC San Diego.

## References

- 1 A. Gupta, J. L. Andresen, R. S. Manan and R. Langer, *Adv. Drug Delivery Rev.*, 2021, **178**, 113834.
- 2 J. A. Kulkarni, D. Witzigmann, S. B. Thomson, S. Chen, B. R. Leavitt, P. R. Cullis and R. van der Meel, *Nat. Nanotechnol.*, 2021, **16**, 630–643.
- 3 N. Lurie, M. Saville, R. Hatchett and J. Halton, *N. Engl. J. Med.*, 2020, **382**, 1969–1973.
- 4 M. Liu, Y. Wang, Y. Zhang, D. Hu, L. Tang, B. Zhou and L. Yang, *Signal Transduction Targeted Ther.*, 2025, **10**, 73.
- 5 X. Sun, S. Setrerrahmane, C. Li, J. Hu and H. Xu, *Signal Transduction Targeted Ther.*, 2024, **9**, 316.
- 6 J. H. Wang, D. J. Gessler, W. Zhan, T. L. Gallagher and G. Gao, *Signal Transduction Targeted Ther.*, 2024, **9**, 78.
- 7 D. Adams, A. Gonzalez-Duarte, W. D. O'Riordan, C. C. Yang, M. Ueda, A. V. Kristen, I. Tournev, H. H. Schmidt, T. Coelho, J. L. Berk, K. P. Lin, G. Vita, S. Attarian, V. Plante-Bordeneuve, M. M. Mezei, J. M. Campistol, J. Buades, T. H. Brannagan 3rd, B. J. Kim, J. Oh, Y. Parman, Y. Sekijima, P. N. Hawkins, S. D. Solomon, M. Polydefkis, P. J. Dyck, P. J. Gandhi, S. Goyal, J. Chen, A. L. Strahs, S. V. Nochur, M. T. Sweetser, P. P. Garg, A. K. Vaishnav, J. A. Gollob and O. B. Suhr, *N. Engl. J. Med.*, 2018, **379**, 11–21.
- 8 A. Lee, *Drugs*, 2025, **85**, 1073–1077.
- 9 X. Bian, L. Zhou, Z. Luo, G. Liu, Z. Hang, H. Li, F. Li and Y. Wen, *ACS Nano*, 2025, **19**, 4039–4083.
- 10 T. Travieso, J. Li, S. Mahesh, J. Mello and M. Blasi, *NPJ Vaccines*, 2022, **7**, 75.
- 11 J. T. Bulcha, Y. Wang, H. Ma, P. W. L. Tai and G. Gao, *Signal Transduction Targeted Ther.*, 2021, **6**, 53.
- 12 A. Srivastava, *Curr. Opin. Virol.*, 2016, **21**, 75–80.
- 13 J. L. Shirley, Y. P. de Jong, C. Terhorst and R. W. Herzog, *Mol. Ther.*, 2020, **28**, 709–722.
- 14 J. A. Greig, K. M. Martins, C. Breton, R. J. Lamontagne, Y. Zhu, Z. He, J. White, J. X. Zhu, J. A. Chichester, Q. Zheng, Z. Zhang, P. Bell, L. Wang and J. M. Wilson, *Nat. Biotechnol.*, 2024, **42**, 1232–1242.
- 15 R. J. Chandler, M. S. Sands and C. P. Venditti, *Hum. Gene Ther.*, 2017, **28**, 314–322.
- 16 Z. Wu, H. Yang and P. Colosi, *Mol. Ther.*, 2010, **18**, 80–86.
- 17 B. Sibbald, *Can. Med. Assoc. J.*, 2001, **164**, 1612.
- 18 A. Lek, B. Wong, A. Keeler, M. Blackwood, K. Ma, S. Huang, K. Sylvia, A. R. Batista, R. Artinian, D. Kokoski, S. Parajuli, J. Putra, C. K. Carreon, H. Lidov, K. Woodman, S. Pajusalu, J. M. Spinazzola, T. Gallagher, J. LaRovere, D. Balderson, L. Black, K. Sutton, R. Horgan, M. Lek and T. Flotte, *N. Engl. J. Med.*, 2023, **389**, 1203–1210.
- 19 D. Duan, *Mol. Ther.*, 2023, **31**, 3123–3126.
- 20 A. S. Meadows, R. J. Pineda, L. Goodchild, T. A. Bobo and H. Fu, *Mol. Ther.-Methods Clin. Dev.*, 2019, **13**, 453–462.
- 21 V. Louis Jeune, J. A. Joergensen, R. J. Hajjar and T. Weber, *Hum. Gene Ther: Methods*, 2013, **24**, 59–67.
- 22 S. Kanvinde, T. Kulkarni, S. Deodhar, D. Bhattacharya and A. Dasgupta, *BioTech*, 2022, **11**, 6.
- 23 C. Wang, C. Pan, H. Yong, F. Wang, T. Bo, Y. Zhao, B. Ma, W. He and M. Li, *J. Nanobiotechnol.*, 2023, **21**, 272.
- 24 M. Ramamoorth and A. Narvekar, *J. Clin. Diagn. Res.*, 2015, **9**, GE01–GE06.
- 25 H. Zhang and M. Barz, *J. Control. Release*, 2025, **381**, 113559.
- 26 J. Wang, Y. Ding, K. Chong, M. Cui, Z. Cao, C. Tang, Z. Tian, Y. Hu, Y. Zhao and S. Jiang, *Vaccines*, 2024, **12**, 1148.
- 27 Y. Zhang, A. Satterlee and L. Huang, *Mol. Ther.*, 2012, **20**, 1298–1304.
- 28 A. B. Hill, M. Chen, C. K. Chen, B. A. Pfeifer and C. H. Jones, *Trends Biotechnol.*, 2016, **34**, 91–105.
- 29 J. Morla-Folch, A. Ranzenigo, Z. A. Fayad and A. J. P. Teunissen, *Small*, 2024, **20**, e2307502.



- 30 X. Du, E. Yada, Y. Terai, T. Takahashi, H. Nakanishi, H. Tanaka, H. Akita and K. Itaka, *Pharmaceutics*, 2023, **15**, 2291.
- 31 R. Mohammadinejad, A. Dehshahri, V. Sagar Madamsetty, M. Zahmatkeshan, S. Tavakol, P. Makvandi, D. Khorsandi, A. Pardakhty, M. Ashrafizadeh, E. Ghasemipour Afshar and A. Zarrabi, *J. Control. Release*, 2020, **325**, 249–275.
- 32 P. Lam and N. F. Steinmetz, *Wiley Interdiscip. Rev.:Nanomed. Nanobiotechnol.*, 2018, **10**, e1487.
- 33 N. F. Steinmetz, *Nanomedicine*, 2010, **6**, 634–641.
- 34 K. B. Scholthof, *Annu. Rev. Phytopathol.*, 2004, **42**, 13–34.
- 35 Y. H. Chung, H. Cai and N. F. Steinmetz, *Adv. Drug Delivery Rev.*, 2020, **156**, 214–235.
- 36 S. Venkataraman and K. Hefferon, *Viruses*, 2021, 13.
- 37 J. Zhang, H. He, F. Zeng, M. Du, D. Huang, G. Chen and Q. Wang, *Adv. NanoBiomed Res.*, 2024, **4**, 2300135.
- 38 S. Eiben, C. Koch, K. Altintoprak, A. Southan, G. Tovar, S. Laschat, I. M. Weiss and C. Wege, *Adv. Drug Delivery Rev.*, 2019, **145**, 96–118.
- 39 N. A. Nikitin, E. A. Trifonova, O. V. Karpova and J. G. Atabekov, *Moscow Univ. Biol. Sci. Bull.*, 2016, **71**, 128–134.
- 40 L. Kan and J. J. Barr, *Annu. Rev. Virol.*, 2023, **10**, 183–198.
- 41 C. Chang, W. Guo, X. Yu, C. Guo, N. Zhou, X. Guo, R. L. Huang, Q. Li and Y. Zhu, *Mater. Today Bio.*, 2023, **20**, 100612.
- 42 K. J. Koudelka, A. S. Pitek, M. Manchester and N. F. Steinmetz, *Annu. Rev. Virol.*, 2015, **2**, 379–401.
- 43 A. Schneemann and M. J. Young, *Adv. Protein Chem.*, 2003, **64**, 1–36.
- 44 G. P. Lomonosoff and D. J. Evans, in *Plant Viral Vectors*, ed. K. Palmer and Y. Gleba, Springer, Berlin, Heidelberg, 2014, vol. 375, pp. 61–87.
- 45 S. B. P. E. Timmermans, A. Ramezani, T. Montalvo, M. Nguyen, P. V. D. Schoot, J. C. M. V. Hest and R. Zandi, *J. Am. Chem. Soc.*, 2022, **144**, 12608–12612.
- 46 A. O. Omole, J. F. Affonso de Oliveira, L. Sutorus, S. Karan, Z. Zhao, B. W. Neun, E. Cedrone, J. D. Clogston, J. Xu, M. Sierk, Q. Chen, D. Meerzaman, M. A. Dobrovolskaia and N. F. Steinmetz, *Commun. Biol.*, 2024, **7**, 1382.
- 47 G. Zahmanova, A. A. Aljabali, K. Takova, V. Toneva, M. M. Tambuwala, A. P. Andonov, G. L. Lukov and I. Minkov, *Int. J. Mol. Sci.*, 2023, **24**, 1533.
- 48 E. P. Rybicki, *Wiley Interdiscip. Rev.:Nanomed. Nanobiotechnol.*, 2020, **12**, e1587.
- 49 P. Opdensteinen, J. F. Affonso de Oliveira, S. Jung and N. F. Steinmetz, *Plant Biotechnol. J.*, 2025, **23**, 5013–5031.
- 50 P. Lam, N. M. Gulati, P. L. Stewart, R. A. Keri and N. F. Steinmetz, *Sci. Rep.*, 2016, **6**, 23803.
- 51 D. J. Hwang, I. M. Roberts and T. M. Wilson, *Arch. Virol. Suppl.*, 1994, **9**, 543–558.
- 52 S. Shukla, C. Wang, V. Beiss, H. Cai, T. Washington 2nd, A. A. Murray, X. Gong, Z. Zhao, H. Masarapu, A. Zlotnick, S. Fiering and N. F. Steinmetz, *Biomater. Sci.*, 2020, **8**, 5489–5503.
- 53 O. Azizgolshani, R. F. Garmann, R. Cadena-Nava, C. M. Knobler and W. M. Gelbart, *Virology*, 2013, **441**, 12–17.
- 54 S. Karan, P. Opdensteinen, Y. Ma, J. F. A. De Oliveira and N. F. Steinmetz, *Vaccine*, 2025, **53**, 127063.
- 55 A. Simms, Z. Zhao, E. Cedrone, M. A. Dobrovolskaia and N. F. Steinmetz, *Bioeng. Transl. Med.*, 2024, **9**, e10693.
- 56 A. Simms, N. Minasov and N. F. Steinmetz, *Nanomedicine*, 2025, **20**, 2425–2431.
- 57 A. S. Pitek, A. M. Wen, S. Shukla and N. F. Steinmetz, *Small*, 2016, **12**, 1758–1769.
- 58 A. Chatterji, W. F. Ochoa, M. Paine, B. R. Ratna, J. E. Johnson and T. Lin, *Chem. Biol.*, 2004, **11**, 855–863.
- 59 A. J. Vaidya and K. V. Solomon, *ACS Appl. Bio Mater.*, 2022, **5**, 1980–1989.
- 60 R. Garcia, S. Latz, J. Romero, G. Higuera, K. Garcia and R. Bastias, *Front. Microbiol.*, 2019, **10**, 1187.
- 61 P. Manohar and N. Ramesh, *Sci. Rep.*, 2019, **9**, 15242.
- 62 J. Mendez, J. Jofre, F. Lucena, N. Contreras, K. Mooijman and R. Araujo, *J. Virol. Methods*, 2002, **106**, 215–224.
- 63 N. Wagner, E. Brinks, M. Samtlebe, J. Hinrichs, Z. Atamer, W. Kot, C. Franz, H. Neve and K. J. Heller, *Int. J. Food Microbiol.*, 2017, **241**, 308–317.
- 64 W. Jaroszewicz, J. Morcinek-Orlowska, K. Pierzynowska, L. Gaffke and G. Wegrzyn, *FEMS Microbiol. Rev.*, 2022, **46**, fuab052.
- 65 P. Tao, M. Mahalingam, B. S. Marasa, Z. Zhang, A. K. Chopra and V. B. Rao, *Proc. Natl. Acad. Sci. U. S. A.*, 2013, **110**, 5846–5851.
- 66 M. V. D. Waterbeemd, J. Snijder, I. B. Tsvetkova, B. G. Dragnea, J. J. Cornelissen and A. J. R. Heck, *J. Am. Soc. Mass Spectrom.*, 2016, **27**, 1000–1009.
- 67 J. A. Speir, S. Munshi, G. Wang, T. S. Baker and J. E. Johnson, *Structure*, 1995, **3**, 63–78.
- 68 A. Diaz-Valle, Y. M. Garcia-Salcedo, G. Chavez-Calvillo, L. Silva-Rosales and M. Carrillo-Tripp, *J. Virol. Methods*, 2015, **225**, 23–29.
- 69 L. Lavelle, J. P. Michel and M. Gingery, *J. Virol. Methods*, 2007, **146**, 311–316.
- 70 R. D. Cadena-Nava, M. Comas-Garcia, R. F. Garmann, A. L. N. Rao, C. M. Knobler and W. M. Gelbart, *J. Virol.*, 2012, **86**, 3318–3326.
- 71 M. Comas-Garcia, R. F. Garmann, S. W. Singaram, A. Ben-Shaul, C. M. Knobler and W. M. Gelbart, *J. Phys. Chem. B*, 2014, **118**, 7510–7519.
- 72 H. Cai, S. Shukla and N. F. Steinmetz, *Adv. Funct. Mater.*, 2020, **30**, 1908743.
- 73 M. Comas-Garcia, R. D. Cadena-Nava, A. L. Rao, C. M. Knobler and W. M. Gelbart, *J. Virol.*, 2012, **86**, 12271–12282.
- 74 S. K. Chan and N. F. Steinmetz, *J. Mater. Chem. B*, 2023, **11**, 816–825.
- 75 M. V. D. Ruiters, R. M. V. D. Hee, A. J. M. Driessen, E. D. Keurhorst, M. Hamid and J. J. L. M. Cornelissen, *J. Control. Release*, 2019, **307**, 342–354.
- 76 C. Pretto, M. Tang, M. Chen, H. Xu, A. Subrizi, A. Urtti and J. C. M. V. Hest, *Macromol. Biosci.*, 2021, **21**, e2100095.
- 77 P. H. Hagedorn, R. Persson, E. D. Funder, N. Albæk, S. L. Diemer, D. J. Hansen, M. R. Møller, N. Papargyri, H. Christiansen, B. R. Hansen, H. F. Hansen,



- M. A. Jensen and T. Koch, *Drug Discovery Today*, 2018, **23**, 101–114.
- 78 S. Mukherjee, C. M. Pfeifer, J. M. Johnson, J. Liu and A. Zlotnick, *J. Am. Chem. Soc.*, 2006, **128**, 2538–2539.
- 79 A. Zlotnick, J. Z. Porterfield and J. C.-Y. Wang, *Biophys. J.*, 2013, **104**, 1595–1604.
- 80 S. J. Maassen, M. V. D. Ruiter, S. Lindhoud and J. J. L. M. Cornelissen, *Chem.–Eur. J.*, 2018, **24**, 7456–7463.
- 81 S. Bauer, C. J. Kirschning, H. Hacker, V. Redecke, S. Hausmann, S. Akira, H. Wagner and G. B. Lipford, *Proc. Natl. Acad. Sci. U. S. A.*, 2001, **98**, 9237–9242.
- 82 J. Vollmer, R. Weeratna, P. Payette, M. Jurk, C. Schetter, M. Laucht, T. Wader, S. Tluk, M. Liu, H. L. Davis and A. M. Krieg, *Eur. J. Immunol.*, 2004, **34**, 251–262.
- 83 C. Pretto and J. C. M. V. Hest, *Bioconj. Chem.*, 2019, **30**, 3069–3077.
- 84 F. Xue, J. J. L. M. Cornelissen, Q. Yuan and S. Cao, *Chin. Chem. Lett.*, 2023, **34**, 107448.
- 85 P. Lam and N. F. Steinmetz, *Biomater. Sci.*, 2019, **7**, 3138–3142.
- 86 A. Nunez-Rivera, P. G. J. Fournier, D. L. Arellano, A. G. Rodriguez-Hernandez, R. Vazquez-Duhalt and R. D. Cadena-Nava, *Beilstein J. Nanotechnol.*, 2020, **11**, 372–382.
- 87 S. Ramos-Carreno, I. Giffard-Mena, J. N. Zamudio-Ocadiz, A. Nunez-Rivera, R. Valencia-Yanez, J. Ruiz-Garcia, M. T. Viana and R. D. Cadena-Nava, *Beilstein J. Org. Chem.*, 2021, **17**, 1360–1373.
- 88 M. V. Villagrana-Escareño, E. Reynaga-Hernández, O. G. Galicia-Cruz, A. L. Durán-Meza, V. D. L. Cruz-González, C. Y. Hernández-Carballo and J. Ruiz-García, *BioMed Res. Int.*, 2019, **2019**, 4630891.
- 89 A. Biddlecome, H. H. Habte, K. M. McGrath, S. Sambanthamoorthy, M. Wurm, M. M. Sykora, C. M. Knobler, I. C. Lorenz, M. Lasaro, K. Elbers and W. M. Gelbart, *PLoS One*, 2019, **14**, e0215031.
- 90 S. Karan, A. L. Duran-Meza, A. Chapman, C. Tanimoto, S. K. Chan, C. M. Knobler, W. M. Gelbart and N. F. Steinmetz, *Mol. Pharm.*, 2024, **21**, 2727–2739.
- 91 J. Mikkilä, A.-P. Eskelinen, E. H. Niemelä, V. Linko, M. J. Frilander, P. Törmä and M. A. Kostiaainen, *Nano Lett.*, 2014, **14**, 2196–2200.
- 92 I. Seitz, S. Saarinen, E. P. Kumpula, D. McNeale, E. Anaya-Plaza, V. Lampinen, V. P. Hytonen, F. Sainsbury, J. Cornelissen, V. Linko, J. T. Huiskonen and M. A. Kostiaainen, *Nat. Nanotechnol.*, 2023, **18**, 1205–1212.
- 93 I. Seitz, S. Saarinen, J. Wierzchowiecka, E.-P. Kumpula, B. Shen, J. J. L. M. Cornelissen, V. Linko, J. T. Huiskonen and M. A. Kostiaainen, *Adv. Mater.*, 2025, **37**, e2417642.
- 94 K. Namba and G. Stubbs, *Science*, 1986, **231**, 1401–1406.
- 95 K. Namba, R. Pattanayek and G. Stubbs, *J. Mol. Biol.*, 1989, **208**, 307–325.
- 96 P. J. Butler, *J. Gen. Virol.*, 1984, **65**, 253–279.
- 97 A. Klug, *Philos. Trans. R. Soc. Lond. B Biol. Sci.*, 1999, **354**, 531–535.
- 98 K. Saunders, E. C. Thuenemann, S. N. Shah, H. Peyret, R. Kristianingsih, S. G. Lopez, J. Richardson and G. P. Lomonosoff, *Front. Bioeng. Biotechnol.*, 2022, **10**, 877361.
- 99 K. E. Richards and R. C. Williams, *Proc. Natl. Acad. Sci. U. S. A.*, 1972, **69**, 1121–1124.
- 100 P. J. Butler and A. Klug, *Nat. New Biol.*, 1971, **229**, 47–50.
- 101 C. Wege and C. Koch, *Wiley Interdiscip. Rev.: Nanomed. Nanobiotechnol.*, 2020, **12**, e1591.
- 102 D. Zimmern, *Cell*, 1977, **11**, 463–482.
- 103 D. R. Gallie, D. E. Sleat, J. W. Watts, P. C. Turner and T. M. Wilson, *Science*, 1987, **236**, 1122–1124.
- 104 K. Saunders and G. P. Lomonosoff, *Front. Plant Sci.*, 2017, **8**, 1335.
- 105 S. Shukla, F. J. Eber, A. S. Nagarajan, N. A. DiFranco, N. Schmidt, A. M. Wen, S. Eiben, R. M. Twyman, C. Wege and N. F. Steinmetz, *Adv. Healthcare Mater.*, 2015, **4**, 874–882.
- 106 F. J. Eber, S. Eiben, H. Jeske and C. Wege, *Angew. Chem., Int. Ed.*, 2013, **52**, 7203–7207.
- 107 M. L. Smith, T. Corbo, J. Bernales, J. A. Lindbo, G. P. Pogue, K. E. Palmer and A. A. McCormick, *Virology*, 2007, **358**, 321–333.
- 108 P. D. Maharaj, J. K. Mallajosyula, G. Lee, P. Thi, Y. Zhou, C. M. Kearney, A. A. McCormick, P. D. Maharaj, J. K. Mallajosyula, G. Lee, P. Thi, Y. Zhou, C. M. Kearney and A. A. McCormick, *Int. J. Mol. Sci.*, 2014, **15**, 18540–18556.
- 109 Y. Zhou, P. D. Maharaj, J. K. Mallajosyula, A. A. McCormick and C. M. Kearney, *Mol. Biotechnol.*, 2015, **57**, 325–336.
- 110 A. A. McCormick, T. A. Corbo, S. Wykoff-Clary, L. V. Nguyen, M. L. Smith, K. E. Palmer and G. P. Pogue, *Vaccine*, 2006, **24**, 6414–6423.
- 111 J. O. Kemnade, M. Seethammagari, M. Collinson-Pautz, H. Kaur, D. M. Spencer and A. A. McCormick, *Vaccine*, 2014, **32**, 4228–4233.
- 112 J. Ou, M. Zhu, X. Ju, D. Xu, G. Lu, K. Li, W. Jiang, C. Wan, Y. Zhao, Y. Han, Y. Tian and Z. Niu, *Nano Lett.*, 2023, **23**, 2056–2064.
- 113 S. Karan, J. F. Affonso De Oliveira, M. A. Moreno-Gonzalez and N. F. Steinmetz, *ACS Appl. Bio Mater.*, 2024, **7**, 7675–7683.
- 114 F. J. Eber, S. Eiben, H. Jeske and C. Wege, *Nanoscale*, 2015, **7**, 344–355.
- 115 A. Schneider, F. J. Eber, N. L. Wenz, K. Altintoprak, H. Jeske, S. Eiben and C. Wege, *Nanoscale*, 2016, **8**, 19853–19866.
- 116 S. Eiben, *Methods Mol. Biol.*, 2018, **1776**, 35–50.
- 117 A. A. McCormick and K. E. Palmer, *Expert Rev. Vaccines*, 2008, **7**, 33–41.
- 118 M. A. Bruckman, X. Yu and N. F. Steinmetz, *Nanotechnology*, 2013, **24**, 462001.
- 119 K. L. Lee, B. L. Carpenter, A. M. Wen, R. A. Ghiladi and N. F. Steinmetz, *ACS Biomater. Sci. Eng.*, 2016, **2**, 838–844.
- 120 M. A. Bruckman, A. E. Czapar, A. VanMeter, L. N. Randolph and N. F. Steinmetz, *J. Control. Release*, 2016, **231**, 103–113.
- 121 M. A. Bruckman, S. Hern, K. Jiang, C. A. Flask, X. Yu and N. F. Steinmetz, *J. Mater. Chem. B*, 2013, **1**, 1482.



- 122 A. A. Caparco, I. González-Gamboa, S. S. Hays, J. K. Pokorski and N. F. Steinmetz, *Nano Lett.*, 2023, **23**, 5785–5793.
- 123 P. Opdensteinen, A. A. Caparco and N. F. Steinmetz, *Mater. Today*, 2025, **88**, 117–128.
- 124 L. Liu, M. C. Cañizares, W. Monger, Y. Perrin, E. Tsakiris, C. Porta, N. Shariat, L. Nicholson and G. P. Lomonosoff, *Vaccine*, 2005, **23**, 1788–1792.
- 125 F. Sainsbury, M. C. Canizares and G. P. Lomonosoff, *Annu. Rev. Phytopathol.*, 2010, **48**, 437–455.
- 126 T. Lin, Z. Chen, R. Usha, C. V. Stauffacher, J. B. Dai, T. Schmidt and J. E. Johnson, *Virology*, 1999, **265**, 20–34.
- 127 Q. Wang, E. Kaltgrad, T. Lin, J. E. Johnson and M. G. Finn, *Chem. Biol.*, 2002, **9**, 805–811.
- 128 H. Peyret and G. P. Lomonosoff, in *Recombinant Proteins in Plants*, ed. S. Schillberg and H. Spiegel, Humana, New York, 2022, vol. 2480, pp. 103–111.
- 129 S. E. Roberts, H. L. Martin, D. Al-Qallaf, A. A. Tang, C. Tiede, T. G. Gaule, A. Dobon-Alonso, R. Overman, S. Shah, H. Peyret, K. Saunders, R. Bon, I. W. Manfield, S. M. Bell, G. P. Lomonosoff, V. Speirs and D. C. Tomlinson, *iScience*, 2024, **27**, 110461.
- 130 H. Peyret, S. N. Shah, Y. Meshcheriakova, J.-W. Jung, K. Saunders and G. P. Lomonosoff, *Plant Biotechnol. J.*, 2025, **24**, 159–170.
- 131 B. Duoto, M. Tong, K. J. Barkovich, J. Schuphan, P. Mali and N. F. Steinmetz, *Sci. Rep.*, 2025, **15**, 43714.
- 132 M. M. Albakri, F. A. Veliz, S. N. Fiering, N. F. Steinmetz and S. F. Sieg, *Immunology*, 2020, **159**, 183–192.
- 133 P. H. Lizotte, A. M. Wen, M. R. Sheen, J. Fields, P. Rojanasopondist, N. F. Steinmetz and S. Fiering, *Nat. Nanotechnol.*, 2016, **11**, 295–303.
- 134 C. Mao, V. Beiss, J. Fields, N. F. Steinmetz and S. Fiering, *Biomaterials*, 2021, **275**, 120914.
- 135 C. Wang, S. N. Fiering and N. F. Steinmetz, *Adv. Ther.*, 2019, **2**, 1900003.
- 136 H. Cai, C. Wang, S. Shukla and N. F. Steinmetz, *Adv. Sci.*, 2019, **6**, 1802281.
- 137 C. Wang and N. F. Steinmetz, *Adv. Funct. Mater.*, 2020, **30**, 2002299.
- 138 S. Shukla, C. Wang, V. Beiss and N. F. Steinmetz, *ACS Nano*, 2020, **14**, 2994–3003.
- 139 J. F. Affonso de Oliveira, S. K. Chan, A. O. Omole, V. Agrawal and N. F. Steinmetz, *ACS Nano*, 2022, **16**, 18315–18328.
- 140 V. Beiss, C. Mao, S. N. Fiering and N. F. Steinmetz, *Mol. Pharm.*, 2022, **19**, 1573–1585.
- 141 A. Kerstetter-Fogle, S. Shukla, C. Wang, V. Beiss, P. L. R. Harris, A. E. Sloan and N. F. Steinmetz, *Cancers*, 2019, **11**, 515.
- 142 P. Sergent, J. C. Pinto-Cardenas, A. J. A. Carrillo, D. L. Davalos, M. D. G. Perez, D. A. M. Lechuga, D. Alonso-Miguel, E. Schaafsma, A. J. Cuarenta, D. C. Munoz, Y. Zarabanda, S. M. Palisoul, P. J. Lewis, F. W. T. Kolling, J. F. Affonso de Oliveira, N. F. Steinmetz, J. L. Rothstein, L. Lines, R. J. Noelle, S. Fiering and H. Arias-Pulido, *Cells*, 2024, **13**, 1478.
- 143 A. Singh, J. F. Affonso de Oliveira, J. Schrader, D. Kishore, S. V. Chandrasekar, S. Fiering, N. F. Steinmetz and A. Ranjan, *Front. Immunol.*, 2025, **16**, 1566394.
- 144 P. Delgado-Bonet, H. Arias-Pulido, N. Del Castillo Magan, A. B. Emilia Zimmermann, E. Schaafsma, J. Vom Berg, F. Vazquez, V. Beiss, N. F. Steinmetz, S. Fiering and A. J. Perise-Barrios, *Mol. Pharm.*, 2025, **22**, 2671–2683.
- 145 G. Valdivia, D. Alonso-Miguel, M. D. Perez-Alenza, A. B. E. Zimmermann, E. Schaafsma, F. W. T. Kolling, L. Barreno, A. Alonso-Diez, V. Beiss, J. F. Affonso de Oliveira, M. Suarez-Redondo, S. Fiering, N. F. Steinmetz, J. Vom Berg, L. Pena and H. Arias-Pulido, *Cells*, 2023, **12**.
- 146 D. Alonso-Miguel, G. Valdivia, D. Guerrero, M. D. Perez-Alenza, S. Pantelyushin, A. Alonso-Diez, V. Beiss, S. Fiering, N. F. Steinmetz, M. Suarez-Redondo, J. Vom Berg, L. Pena and H. Arias-Pulido, *J. Immunother. Cancer*, 2022, **10**, e004044.
- 147 P. J. Hoopes, R. J. Wagner, K. Duval, K. Kang, D. J. Gladstone, K. L. Moodie, M. Crary-Burney, H. Ariaspulido, F. A. Veliz, N. F. Steinmetz and S. N. Fiering, *Mol. Pharm.*, 2018, **15**, 3717–3722.
- 148 A. O. Omole, H. S. Newton, E. Cedrone, K. Nematpour, S. Xie, Y. Zhao, B. Tran, M. A. Dobrovolskaia and N. F. Steinmetz, *Cells Biomater.*, 2025, **1**, 100095.
- 149 C. Mao, V. Beiss, G. W. Ho, J. Fields, N. F. Steinmetz and S. Fiering, *J. Immunother. Cancer*, 2022, **10**, e005834.
- 150 N. Sonenberg, A. J. Shatkin, R. P. Ricciardi, M. Rubin and R. M. Goodman, *Nucleic Acids Res.*, 1978, **5**, 2501–2512.
- 151 C. Lico, E. Benvenuto and S. Baschieri, *Front. Plant Sci.*, 2015, **6**, 1009.
- 152 D. H. T. Le, H. Hu, U. Commandeur and N. F. Steinmetz, *J. Struct. Biol.*, 2017, **200**, 360–368.
- 153 S. J. Kwon, M. R. Park, K. W. Kim, C. A. Plante, C. L. Hemenway and K. H. Kim, *Virology*, 2005, **334**, 83–97.
- 154 S. S. Krishna, C. N. Hiremath, S. K. Munshi, D. Prahadeeswaran, M. Sastri, H. S. Savithri and M. R. Murthy, *J. Mol. Biol.*, 1999, **289**, 919–934.
- 155 H. Hu, H. Masarapu, Y. Gu, Y. Zhang, X. Yu and N. F. Steinmetz, *ACS Appl. Mater. Interfaces*, 2019, **11**, 18213–18223.
- 156 H. Masarapu, B. K. Patel, P. L. Chariou, H. Hu, N. M. Gulati, B. L. Carpenter, R. A. Ghiladi, S. Shukla and N. F. Steinmetz, *Biomacromolecules*, 2017, **18**, 4141–4153.
- 157 M. Sastri, R. Kekuda, K. Gopinath, C. T. Kumar, J. R. Jagath and H. S. Savithri, *J. Mol. Biol.*, 1997, **272**, 541–552.
- 158 H. Hu and N. F. Steinmetz, *Cancers*, 2021, **13**, 2909.
- 159 X. Wang and P. Ahlquist, in *Encyclopedia of Virology*, ed. B. W. J. Mahy and M. H. V. V. Regenmortel, Academic Press, Boston, 3rd edn, 2008, pp. 381–386.
- 160 Z. Wang, C. F. Hryc, B. Bammes, P. V. Afonine, J. Jakana, D. H. Chen, X. Liu, M. L. Baker, C. Kao, S. J. Ludtke, M. F. Schmid, P. D. Adams and W. Chiu, *Nat. Commun.*, 2014, **5**, 4808.
- 161 A. Strugała, J. Jagielski, K. Kamel, G. Nowaczyk, M. Radom, M. Figlerowicz, A. Urbanowicz, A. Strugała, J. Jagielski, K. Kamel, G. Nowaczyk, M. Radom, M. Figlerowicz and A. Urbanowicz, *Int. J. Mol. Sci.*, 2021, **22**, 3098.



- 162 R. Golmohammadi, K. Valegard, K. Fridborg and L. Liljas, *J. Mol. Biol.*, 1993, **234**, 620–639.
- 163 P. G. Stockley, N. J. Stonehouse and K. Valegard, *Int. J. Biochem.*, 1994, **26**, 1249–1260.
- 164 G. G. Pickett and D. S. Peabody, *Nucleic Acids Res.*, 1993, **21**, 4621–4626.
- 165 B. Wei, Y. Wei, K. Zhang, J. Wang, R. Xu, S. Zhan, G. Lin, W. Wang, M. Liu, L. Wang, R. Zhang and J. Li, *Biomed. Pharmacother.*, 2009, **63**, 313–318.
- 166 P. T. Lowary and O. C. Uhlenbeck, *Nucleic Acids Res.*, 1987, **15**, 10483–10493.
- 167 S. Zhan, J. Li, R. Xu, L. Wang, K. Zhang and R. Zhang, *J. Clin. Microbiol.*, 2009, **47**, 2571–2576.
- 168 G. W. Witherell, H. N. Wu and O. C. Uhlenbeck, *Biochemistry*, 1990, **29**, 11051–11057.
- 169 G. Zhou, Z. Luo, Z. Zhang, S. Cao and Y. Li, *Front. Immunol.*, 2025, **16**, 1651594.
- 170 A. Naskalska and J. G. Heddle, *Nanomedicine*, 2024, **19**, 1103–1115.
- 171 Y. Fu and J. Li, *Virus Res.*, 2016, **211**, 9–16.
- 172 Y. Pan, Y. Zhang, T. Jia, K. Zhang, J. Li and L. Wang, *FEBS J.*, 2012, **279**, 1198–1208.
- 173 D. Legendre and J. Fastrez, *J. Biotechnol.*, 2005, **117**, 183–194.
- 174 S. Sun, W. Li, Y. Sun, Y. Pan and J. Li, *Biochem. Biophys. Res. Commun.*, 2011, **407**, 124–128.
- 175 C. Ma, M. Yang, W. Zhou, S. Guo, H. Zhang, J. Gong, X. E. Zhang and F. Li, *Nano Lett.*, 2025, **25**, 3038–3044.
- 176 L. Zhang, Y. Sun, L. Chang, T. Jia, G. Wang, R. Zhang, K. Zhang and J. Li, *Appl. Microbiol. Biotechnol.*, 2015, **99**, 7047–7057.
- 177 J. Li, Y. Sun, T. Jia, R. Zhang, K. Zhang and L. Wang, *Int. J. Cancer*, 2014, **134**, 1683–1694.
- 178 Y. Pan, T. Jia, Y. Zhang, K. Zhang, R. Zhang, J. Li and L. Wang, *Int. J. Nanomed.*, 2012, **7**, 5957–5967.
- 179 Y. Yao, T. Jia, Y. Pan, H. Gou, Y. Li, Y. Sun, R. Zhang, K. Zhang, G. Lin, J. Xie, J. Li and L. Wang, *Int. J. Mol. Sci.*, 2015, **16**, 8337–8350.
- 180 J. Zhang, D. Li, R. Zhang, R. Peng, J. Li, D. L. Jiawei Zhang, R. Zhang, R. Peng and J. Li, *Exp. Biol. Med.*, 2021, **246**, 2463–2472.
- 181 G. Wang, T. Jia, X. Xu, L. Chang, R. Zhang, Y. Fu, Y. Li, X. Yang, K. Zhang, G. Lin, Y. Han and J. Li, *Oncotarget*, 2016, **7**, 59402–59416.
- 182 R. A. Mastico, S. J. Talbot and P. G. Stockley, *J. Gen. Virol.*, 1993, **74**(Pt 4), 541–548.
- 183 F. A. Galaway and P. G. Stockley, *Mol. Pharm.*, 2013, **10**, 59–68.
- 184 C. E. Ashley, E. C. Carnes, G. K. Phillips, P. N. Durfee, M. D. Buley, C. A. Lino, D. P. Padilla, B. Phillips, M. B. Carter, C. L. Willman, C. J. Brinker, J. D. Caldeira, B. Chackerian, W. Wharton and D. S. Peabody, *ACS Nano*, 2011, **5**, 5729–5745.
- 185 M. Wu, T. Sherwin, W. L. Brown and P. G. Stockley, *Nanomedicine*, 2005, **1**, 67–76.
- 186 M. A. Crone and P. S. Freemont, *GEN Biotechnol.*, 2022, **1**, 496–503.
- 187 M. Wu, W. L. Brown and P. G. Stockley, *Bioconj. Chem.*, 1995, **6**, 587–595.
- 188 K. Hashemi, M. M. Ghahramani Seno, M. R. Ahmadian, B. Malaekhe-Nikouei, M. R. Bassami, H. Dehghani and A. Afkhami-Goli, *Sci. Rep.*, 2021, **11**, 19851.
- 189 A. P. Biela, A. Naskalska, F. Fatehi, R. Twarock and J. G. Heddle, *Commun. Mater.*, 2022, **3**, 7.
- 190 A. Naskalska, M. Walczak, A. Dabrowska, M. Bochenek, A. Biela and J. Heddle, *Int. J. Pharm.*, 2025, **682**, 125865.
- 191 Y. Knopp, F. K. Geis, D. Heckl, S. Horn, T. Neumann, J. Kuehle, J. Meyer, B. Fehse, C. Baum, M. Morgan, J. Meyer, A. Schambach and M. Galla, *Mol. Ther.-Nucleic Acids*, 2018, **13**, 256–274.
- 192 Y. Baron, J. Sens, L. Lange, L. Nassauer, D. Klatt, D. Hoffmann, M. J. Kleppa, P. V. Barbosa, M. Keisker, V. Steinberg, J. D. Suerth, F. W. R. Vondran, J. Meyer, M. Morgan, A. Schambach and M. Galla, *Mol. Ther.-Nucleic Acids*, 2022, **27**, 810–823.
- 193 S. Ling, S. Yang, X. Hu, D. Yin, Y. Dai, X. Qian, D. Wang, X. Pan, J. Hong, X. Sun, H. Yang, S. R. Paludan and Y. Cai, *Nat. Biomed. Eng.*, 2021, **5**, 144–156.
- 194 S. Ling, X. Zhang, Y. Dai, Z. Jiang, X. Zhou, S. Lu, X. Qian, J. Liu, N. Selfjord, T. M. Satir, A. Lundin, J. L. Touza, M. Firth, N. Van Zuydam, B. Bilican, P. Akcakaya, J. Hong and Y. Cai, *Nat. Nanotechnol.*, 2025, **20**, 543–553.
- 195 D. Yin, S. Ling, D. Wang, Y. Dai, H. Jiang, X. Zhou, S. R. Paludan, J. Hong and Y. Cai, *Nat. Biotechnol.*, 2021, **39**, 567–577.
- 196 R. Golmohammadi, K. Fridborg, M. Bundule, K. Valegard and L. Liljas, *Structure*, 1996, **4**, 543–554.
- 197 B. C. Bundy and J. R. Swartz, *J. Biotechnol.*, 2011, **154**, 230–239.
- 198 M. O. Mohsen, M. Vogel, C. Riether, J. Muller, S. Salatino, N. Ternette, A. C. Gomes, G. Cabral-Miranda, A. El-Turabi, C. Ruedl, T. M. Kundig, S. Dermime, A. Knuth, D. E. Speiser and M. F. Bachmann, *Front. Immunol.*, 2019, **10**, 1015.
- 199 I. Cielens, V. Ose, I. Petrovskis, A. Strelnikova, R. Renhofa, T. Kozlovska and P. Pumpens, *FEBS Lett.*, 2000, **482**, 261–264.
- 200 T. Storni, C. Ruedl, K. Schwarz, R. A. Schwendener, W. A. Renner and M. F. Bachmann, *J. Immunol.*, 2004, **172**, 1777–1785.
- 201 M. O. Mohsen, D. E. Speiser, J. Michaux, H. S. Pak, B. J. Stevenson, M. Vogel, V. P. Inchakalody, S. d. Brot, S. Dermime, G. Coukos, M. Bassani-Sternberg and M. F. Bachmann, *J. Immunother. Cancer*, 2022, **10**, e002927.
- 202 S. M. Goldinger, R. Dummer, P. Baumgaertner, D. Mihic-Probst, K. Schwarz, A. Hammann-Haenni, J. Willers, C. Geldhof, J. O. Prior, T. M. Kundig, O. Michielin, M. F. Bachmann and D. E. Speiser, *Eur. J. Immunol.*, 2012, **42**, 3049–3061.
- 203 A. Ribas, T. Medina, J. M. Kirkwood, Y. Zakharia, R. Gonzalez, D. Davar, B. Chmielowski, K. M. Campbell, R. Bao, H. Kelley, A. Morris, D. Mauro, J. E. Wooldridge, J. J. Luke, G. J. Weiner, A. M. Krieg and M. M. Milhem, *Cancer Discov.*, 2021, **11**, 2998–3007.



- 204 D. Davar, R. M. Morrison, A. K. Dzutsev, A. Karunamurthy, J. M. Chauvin, F. Amatore, J. S. Deutsch, R. X. Das Neves, R. R. Rodrigues, J. A. McCulloch, H. Wang, D. J. Hartman, J. H. Badger, M. R. Fernandes, Y. Bai, J. Sun, A. M. Cole, P. Aggarwal, J. R. Fang, C. Deitrick, R. Bao, U. Duvvuri, S. S. Sridharan, S. W. Kim, A. C. H, M. P. Holtzman, J. F. Pingpank, J. P. O'Toole, R. DeBlasio, Y. Jin, Q. Ding, W. Gao, C. Groetsch, O. Pagliano, A. Rose, C. Urban, J. Singh, P. Divarkar, D. Mauro, D. Bobilev, J. Wooldridge, A. M. Krieg, M. G. Fury, J. R. Whiteaker, L. Zhao, A. G. Paulovich, Y. G. Najjar, J. J. Luke, J. M. Kirkwood, J. M. Taube, H. J. Park, G. Trinchieri and H. M. Zarour, *Cancer Cell*, 2024, **42**, 1898–1918.
- 205 Y. Cheng, C. D. Lemke-Miltner, W. Wongpattaraworakul, Z. Wang, C. H. F. Chan, A. K. Salem, G. J. Weiner and A. L. Simons, *J. Immunother. Cancer*, 2020, **8**, e000940.
- 206 C. D. Lemke-Miltner, S. E. Blackwell, C. Yin, A. E. Krug, A. J. Morris, A. M. Krieg and G. J. Weiner, *J. Immunol.*, 2020, **204**, 1386–1394.
- 207 L. Vuitika, N. Cortes, V. B. Malaquias, J. D. Q. Silva, A. Lira, W. A. Prates-Syed, L. F. Schimke, D. Luz, R. Duraes-Carvalho, A. Balan, N. O. S. Camara, O. Cabral-Marques, J. E. Krieger, M. H. Hirata and G. Cabral-Miranda, *Sci. Rep.*, 2024, **14**, 24228.
- 208 N. Cortes, A. Lira, J. D. Q. Silva, E. Carvalho, W. A. Prates-Syed, B. Hamaguchi, R. Duraes-Carvalho, A. Balan, N. O. S. Camara, O. Cabral-Marques, N. Pardi, E. C. Sabino, J. E. Krieger and G. Cabral-Miranda, *NPJ Vaccines*, 2025, **10**, 107.
- 209 H. H. Pang, C. Y. Huang, Y. W. Chou, C. J. Lin, Z. L. Zhou, Y. L. Shiue, K. C. Wei and H. W. Yang, *Nanoscale*, 2019, **11**, 8102–8109.
- 210 L. M. Hagge, A. Shahriarkevisahi, N. M. Al-Kharji, Z. Chen, O. R. Brohlin, I. Trashi, A. Tumas, C. H. F, A. V. Adlooru, H. Lee, H. R. Firouzi, S. A. Cornelius, N. J. De Nisco and J. J. Gassensmith, *J. Mater. Chem. B*, 2023, **11**, 7126–7133.
- 211 H.-H. Pang, C.-Y. Huang, P.-Y. Chen, N.-S. Li, Y.-P. Hsu, J.-K. Wu, H.-F. Fan, K.-C. Wei and H.-W. Yang, *ACS Nano*, 2023, **17**, 10407–10422.
- 212 P. M. van Wezenbeek, T. J. Hulsebos and J. G. Schoenmakers, *Gene*, 1980, **11**, 129–148.
- 213 R. Wang, H. D. Li, Y. Cao, Z. Y. Wang, T. Yang and J. H. Wang, *Anal. Bioanal. Chem.*, 2023, **415**, 3927–3944.
- 214 G. P. Smith, *Science*, 1985, **228**, 1315–1317.
- 215 D. Larocca, A. Witte, W. Johnson, G. F. Pierce and A. Baird, *Hum. Gene Ther.*, 1998, **9**, 2393–2399.
- 216 M. A. Poul and J. D. Marks, *J. Mol. Biol.*, 1999, **288**, 203–211.
- 217 L. Urbanelli, C. Ronchini, L. Fontana, S. Menard, R. Orlandi and P. Monaci, *J. Mol. Biol.*, 2001, **313**, 965–976.
- 218 W. Jechlinger, *Expert Rev. Vaccines*, 2006, **5**, 803–825.
- 219 Z. Y. Chen, C. Y. He, L. Meuse and M. A. Kay, *Gene Ther.*, 2004, **11**, 856–864.
- 220 S. Wong, S. Jimenez and R. A. Slavcev, *Microb. Cell Fact.*, 2023, **22**, 124.
- 221 S. Wong, S. Jimenez, D. Pushparajah, R. Prakash and R. Slavcev, *Mol. Ther.-Nucleic Acids*, 2025, **36**, 102571.
- 222 C. Y. Kao, Y. C. Pan, Y. H. Hsiao, S. K. Lim, T. W. Cheng, S. W. Huang, S. M. Wu, C. P. Sun, M. H. Tao and K. Y. Mou, *ACS Nano*, 2023, **17**, 14532–14544.
- 223 U. Tsedev, C. W. Lin, G. T. Hess, J. N. Sarkaria, F. C. Lam and A. M. Belcher, *ACS Nano*, 2022, **16**, 11676–11691.
- 224 A. Hajitou, M. Trepel, C. E. Lilley, S. Soghomonyan, M. M. Alauddin, F. C. Marini 3rd, B. H. Restel, M. G. Ozawa, C. A. Moya, R. Rangel, Y. Sun, K. Zaoui, M. Schmidt, C. von Kalle, M. D. Weitzman, J. G. Gelovani, R. Pasqualini and W. Arap, *Cell*, 2006, **125**, 385–398.
- 225 S. Y. Yoo, H. E. Jin, D. S. Choi, M. Kobayashi, Y. Farouz, S. Wang and S. W. Lee, *Adv. Healthcare Mater.*, 2016, **5**, 88–93.
- 226 K. Suwan, T. Yata, S. Waramit, J. M. Przystal, C. A. Stoneham, K. Bentayebi, P. Asavarut, A. Chongchai, P. Pothachareon, K.-Y. Lee, S. Topanurak, T. L. Smith, J. G. Gelovani, R. L. Sidman, R. Pasqualini, W. Arap and A. Hajitou, *Proc. Natl. Acad. Sci. U. S. A.*, 2019, **116**, 18571–18577.
- 227 A. Chongchai, S. Waramit, K. Suwan, M. Al-Bahrani, S. Udomruk, T. Phitak, P. Kongtawelert, P. Pothachareon and A. Hajitou, *FASEB J.*, 2021, **35**, e21487.
- 228 P. Asavarut, S. Waramit, K. Suwan, G. J. K. Marais, A. Chongchai, S. Benjathummarak, M. Al-Bahrani, P. Vila-Gomez, M. Williams, P. Kongtawelert, T. Yata and A. Hajitou, *EMBO Mol. Med.*, 2022, **14**, e15418.
- 229 L. Gay, K. Suwan and A. Hajitou, *Nat. Protoc.*, 2024, 1–44.
- 230 P. Sittiju, B. Wudtiwai, A. Chongchai, A. Hajitou, P. Kongtawelert, P. Pothachareon and K. Suwan, *Nanoscale*, 2024, **16**, 6603–6617.
- 231 S. Hashiguchi, Y. Yamaguchi, O. Takeuchi, S. Akira and K. Sugimura, *Biochem. Biophys. Res. Commun.*, 2010, **402**, 19–22.
- 232 S. Huang, Y. He, A. Madow, H. Peng, M. Griffin, J. Qi, M. Huang, H. Amoroso, R. Abrashoff, N. Heldman and A. M. Belcher, *Adv. Mater.*, 2025, **37**, e10229.
- 233 X. Dong, P. Pan, J. J. Ye, Q. L. Zhang and X. Z. Zhang, *Biomaterials*, 2022, **289**, 121763.
- 234 T. Yata, K.-Y. Lee, T. Dharakul, S. Songsivilai, A. Bismarck, P. J. Mintz and A. Hajitou, *Mol. Ther.-Nucleic Acids*, 2014, **3**, e185.
- 235 F. Wang, S. Chen, Y. Xia, C. Liu, Z. Xu, R. Song, W. Liu, T. Liu, G. Chen and Q. Liu, *ACS Appl. Mater. Interfaces*, 2025, **17**, 419–429.
- 236 Y. Suzuki, T. Ishimoto, S. Fujita, S. Kiryu, M. Wada, T. Akatsuka, M. Saito and M. Kawano, *Biochem. Biophys. Res. Commun.*, 2020, **530**, 533–540.
- 237 K. N. Lam, P. Spanogiannopoulos, P. Soto-Perez, M. Alexander, M. J. Nalley, J. E. Bisanz, R. R. Nayak, A. M. Weakley, F. B. Yu and P. J. Turnbaugh, *Cell Rep.*, 2021, **37**, 109930.
- 238 P. G. Leiman, S. Kanamaru, V. V. Mesyanzhinov, F. Arisaka and M. G. Rossmann, *Cell. Mol. Life Sci.*, 2003, **60**, 2356–2370.
- 239 V. B. Rao, A. Fokine, Q. Fang and Q. Shao, *Viruses*, 2023, **15**, 527.



- 240 D. N. Fuller, D. M. Raymer, V. I. Kottadiel, V. B. Rao and D. E. Smith, *Proc. Natl. Acad. Sci. U. S. A.*, 2007, **104**, 16868–16873.
- 241 J. Zhu, N. Ananthaswamy, S. Jain, H. Batra, W.-C. Tang, D. A. Lewry, M. L. Richards, S. A. David, P. B. Kilgore, J. Sha, A. Drelich, C.-T. K. Tseng, A. K. Chopra and V. B. Rao, *Sci. Adv.*, 2021, **7**, eabh1547.
- 242 J. Zhu, H. Batra, N. Ananthaswamy, M. Mahalingam, P. Tao, X. Wu, W. Guo, A. Fokine and V. B. Rao, *Nat. Commun.*, 2023, **14**, 2928.
- 243 J. Zhu, P. Tao, M. Mahalingam, J. Sha, P. Kilgore, A. K. Chopra and V. Rao, *Sci. Adv.*, 2019, **5**, eaax0064.
- 244 Z. R. Baker, Y. Zhang, H. Zhang, H. C. Franklin, P. B. S. Serpa, T. Southard, L. Li and B. B. Hsu, *Nat. Biotechnol.*, 2025, 1–10.
- 245 X. L. Hou, B. Zhang, K. Cheng, F. Zhang, X. T. Xie, W. Chen, L. F. Tan, J. X. Fan, B. Liu and Q. R. Xu, *Adv. Sci.*, 2024, **11**, e2308349.
- 246 T. Hohn and I. Katsura, in *Current Topics in Microbiology and Immunology*, ed. W. Arber, W. Henle, P. H. Hofschneider, J. H. Humphrey, J. Klein, P. Koldovský, H. Koprowski, O. Maaløe, F. Melchers, R. Rott, H. G. Schweiger, L. Syruček and P. K. Vogt, Springer, Berlin, Heidelberg, 1977, vol. 78, pp. 69–110.
- 247 C. K. Lee, H. J. Lee, S. H. Jeong and S. J. Lee, *Front. Microbiol.*, 2025, **16**, 1575339.
- 248 B. B. Hsu, I. N. Plant, L. Lyon, F. M. Anastassacos, J. C. Way and P. A. Silver, *Nat. Commun.*, 2020, **11**, 5030.
- 249 B. E. Rubin, S. Diamond, B. F. Cress, A. Crits-Christoph, Y. C. Lou, A. L. Borges, H. Shivram, C. He, M. Xu, Z. Zhou, S. J. Smith, R. Rovinsky, D. C. J. Smock, K. Tang, T. K. Owens, N. Krishnappa, R. Sachdeva, R. Barrangou, A. M. Deutschbauer, J. F. Banfield and J. A. Doudna, *Nat. Microbiol.*, 2022, **7**, 34–47.
- 250 C. D. Jepson and J. B. March, *Vaccine*, 2004, **22**, 2413–2419.
- 251 J. Collins and B. Hohn, *Proc. Natl. Acad. Sci. U. S. A.*, 1978, **75**, 4242–4246.
- 252 C. R. Merrill, M. R. Geier and J. C. Petricciani, *Nature*, 1971, **233**, 398–400.
- 253 I. S. Dunn, *Biochimie*, 1996, **78**, 856–861.
- 254 S. Piersanti, G. Cherubini, Y. Martina, B. Salone, D. Avitabile, F. Grosso, E. Cundari, G. Di Zenzo and I. Saggio, *J. Mol. Med.*, 2004, **82**, 467–476.
- 255 H. A. Lankes, C. N. Zanghi, K. Santos, C. Capella, C. M. Duke and S. Dewhurst, *J. Appl. Microbiol.*, 2007, **102**, 1337–1349.
- 256 J. R. Clark and J. B. March, *FEMS Immunol. Med. Microbiol.*, 2004, **40**, 21–26.
- 257 J. B. March, J. R. Clark and C. D. Jepson, *Vaccine*, 2004, **22**, 1666–1671.
- 258 J. R. Clark, K. Bartley, C. D. Jepson, V. Craik and J. B. March, *FEMS Immunol. Med. Microbiol.*, 2011, **61**, 197–204.
- 259 A. Ghaemi, H. Soleimanjahi, P. Gill, Z. Hassan, S. R. Jahromi and F. Roohvand, *Genet. Vaccines Ther.*, 2010, **8**, 3.
- 260 A. Shoaee-Hassani, P. Keyhanvar, A. M. Seifalian, S. A. Mortazavi-Tabatabaei, N. Ghaderi, K. Issazadeh, N. Amirmozafari and J. Verdi, *PLoS One*, 2013, **8**, e79907.
- 261 F. Y. Li, X. E. Tan, Y. Shimamori, K. Kiga, S. Veeranarayanan, S. Watanabe, Y. Nishikawa, Y. Aiba, Y. Sato'o, K. Miyanaga, T. Sasahara, S. Hossain, K. Thitiananpakorn, T. Kawaguchi, H. M. Nguyen, A. Yeo Syin Lian, S. Sultana, O. Alessa, G. Kumwenda, J. Sarangi, J. E. C. Revilleza, P. Baranwal, M. O. Faruk, Y. Hidaka, M. Thu, M. Arbaah, A. Batbold, Maniruzzaman, Y. Liu, H. T. M. Duyen, T. Sugano, N. Tergel, T. Shimojojo and L. Cui, *Commun. Biol.*, 2024, **7**, 1129.
- 262 Y. W. Huan, V. Torraca, R. Brown, J. Fa-arun, S. L. Miles, D. A. Oyarzún, S. Mostowy and B. Wang, *ACS Synth. Biol.*, 2023, **12**, 709–721.
- 263 N. Nittayasut, T. Yata, S. Chirakul, N. Techakriengkrai and P. Chanchaithong, *PLoS One*, 2024, **19**, e0303555.
- 264 Y. Sun, Y. Sun and R. Zhao, *J. Biosci. Bioeng.*, 2017, **124**, 242–249.
- 265 S. Qazi, H. M. Miettinen, R. A. Wilkinson, K. McCoy, T. Douglas and B. Wiedenheft, *Mol. Pharm.*, 2016, **13**, 1191–1196.
- 266 Z. Li, L. Zhang, K. Jiang, Y. Zhang, Y. Liu, G. Hu and J. Song, *Biosafety and Health*, 2022, **4**, 105–117.
- 267 Y. Lee, M. Jeong, J. Park, H. Jung and H. Lee, *Exp. Mol. Med.*, 2023, **55**, 2085–2096.
- 268 R. Wallace, C. M. Bliss and A. L. Parker, *Viruses*, 2024, **16**.
- 269 C. I. Nkanga and N. F. Steinmetz, *Virology*, 2021, **556**, 39–61.
- 270 S. T. Stern, J. F. Affonso de Oliveira, J. Gatus, E. Edmondson, B. W. Neun, M. A. Dobrovolskaia and N. F. Steinmetz, *Toxicol Rep*, 2025, **14**, 102022.
- 271 P. Singh, D. Prasuhn, R. M. Yeh, G. Destito, C. S. Rae, K. Osborn, M. G. Finn and M. Manchester, *J. Control. Release*, 2007, **120**, 41–50.
- 272 C. R. Kaiser, M. L. Flenniken, E. Gillitzer, A. L. Harmsen, A. G. Harmsen, M. A. Jutila, T. Douglas and M. J. Young, *Int. J. Nanomed.*, 2007, **2**, 715–733.
- 273 A. Blandino, C. Lico, S. Baschieri, L. Barberini, C. Cirotto, P. Blasi and L. Santi, *Colloids Surf., B*, 2015, **129**, 130–136.
- 274 L. Li, L. Wang, R. Xiao, G. Zhu, Y. Li, C. Liu, R. Yang, Z. Tang, J. Li, W. Huang, L. Chen, X. Zheng, Y. He and J. Tan, *Biosci. Rep.*, 2012, **32**, 171–186.
- 275 A. A. Murray, C. Wang, S. Fiering and N. F. Steinmetz, *Mol. Pharm.*, 2018, **15**, 3700–3716.
- 276 A. S. Pitek, S. A. Jameson, F. A. Veliz, S. Shukla and N. F. Steinmetz, *Biomaterials*, 2016, **89**, 89–97.
- 277 H. Bludau, A. E. Czapar, A. S. Pitek, S. Shukla, R. Jordan and N. F. Steinmetz, *Eur. Polym. J.*, 2017, **88**, 679–688.
- 278 N. M. Gulati, A. S. Pitek, N. F. Steinmetz and P. L. Stewart, *Nanoscale*, 2017, **9**, 3408–3415.
- 279 M. Shahgolzari and S. Fiering, *J. Cancer Immunol.*, 2022, **4**, 22–29.
- 280 N. M. Hitchcock, D. Devequi Gomes Nunes, J. Shiach, K. Valeria Saraiva Hodel, J. Dantas Viana Barbosa, L. Alencar Pereira Rodrigues, B. S. Coler, M. Botelho Pereira Soares and R. Badaro, *Viruses*, 2023, **15**, 1020.



- 281 M. C. Bichet, W. H. Chin, W. Richards, Y.-W. Lin, L. Avellaneda-Franco, C. A. Hernandez, A. Oddo, O. Chernyavskiy, V. Hilsenstein, A. Neild, J. Li, N. H. Voelcker, R. Patwa and J. J. Barr, *iScience*, 2021, **24**, 102287.
- 282 K. Bodner, A. L. Melkonian and M. W. Covert, *Trends Microbiol.*, 2021, **29**, 528–541.
- 283 M. Podlacha, L. Gaffke, L. Grabowski, J. Mantej, M. Grabski, M. Pierzchalska, K. Pierzynowska, G. Wegrzyn and A. Wegrzyn, *Nat. Commun.*, 2024, **15**, 2274.
- 284 K. Dabrowska, P. Miernikiewicz, A. Piotrowicz, K. Hodyra, B. Owczarek, D. Lecion, Z. Kazmierczak, A. Letarov and A. Gorski, *J. Virol.*, 2014, **88**, 12551–12557.
- 285 K. Mori, T. Kubo, Y. Kibayashi, T. Ohkuma and A. Kaji, *Antiviral Res.*, 1996, **31**, 79–86.
- 286 R. Sartorius, L. D'Apice, M. Trovato, F. Cuccaro, V. Costa, M. G. D. Leo, V. M. Marzullo, C. Biondo, S. D'Auria, M. A. D. Matteis, A. Ciccodicola and P. D. Berardinis, *EMBO Mol. Med.*, 2015, **7**, 973–988.
- 287 L. Han, X. Guo, C. Xu, W. Shen and Z. Zhao, *Biochem. Biophys. Res. Commun.*, 2024, **712–713**, 149915.
- 288 S. Nooraei, H. Bahrulolum, Z. S. Hoseini, C. Katalani, A. Hajizade, A. J. Easton, G. Ahmadian, S. Nooraei, H. Bahrulolum, Z. S. Hoseini, C. Katalani, A. Hajizade, A. J. Easton and G. Ahmadian, *J. Nanobiotechnol.*, 2021, **19**, 59.
- 289 C. M. Carmody, J. M. Goddard and S. R. Nugen, *Bioconj. Chem.*, 2021, **32**, 466–481.
- 290 M. Asmamaw Mengstie, *Front Bioeng. Biotechnol.*, 2022, **10**, 895713.
- 291 Y. Wang, H. Jiang, M. Li, Z. Xu, H. Xu, Y. Chen, K. Chen, W. Zheng, W. Lin, Z. Liu, Z. Lin and M. Zhang, *Gene*, 2024, **927**, 148733.
- 292 J. Han, H. Bai, F. Li, Y. Zhang, Q. Zhou and W. Li, *Nat. Commun.*, 2025, **16**, 9157.
- 293 Y. Sun, S. Chatterjee, X. Lian, Z. Traylor, S. R. Sattiraju, Y. Xiao, S. A. Dilliard, Y. C. Sung, M. Kim, S. M. Lee, S. Moore, X. Wang, D. Zhang, S. Wu, P. Basak, J. Wang, J. Liu, R. J. Mann, D. F. LePage, W. Jiang, S. Abid, M. Hennig, A. Martinez, B. A. Wustman, D. J. Lockhart, R. Jain, R. A. Conlon, M. L. Drumm, C. A. Hodges and D. J. Siegart, *Science*, 2024, **384**, 1196–1202.
- 294 Q. Cheng, T. Wei, L. Farbiak, L. T. Johnson, S. A. Dilliard and D. J. Siegart, *Nat. Nanotechnol.*, 2020, **15**, 313–320.
- 295 K. Chen, H. Han, S. Zhao, B. Xu, B. Yin, A. Lawanprasert, M. Trinidad, B. W. Burgstone, N. Murthy and J. A. Doudna, *Nat. Biotechnol.*, 2025, **43**, 1445–1457.
- 296 S. Banskota, A. Raguram, S. Suh, S. W. Du, J. R. Davis, E. H. Choi, X. Wang, S. C. Nielsen, G. A. Newby, P. B. Randolph, M. J. Osborn, K. Musunuru, K. Palczewski and D. R. Liu, *Cell*, 2022, **185**, 250–265.
- 297 M. An, A. Raguram, S. W. Du, S. Banskota, J. R. Davis, G. A. Newby, P. Z. Chen, K. Palczewski and D. R. Liu, *Nat. Biotechnol.*, 2024, **42**, 1526–1537.
- 298 A. Raguram, M. An, P. Z. Chen and D. R. Liu, *Nat. Biotechnol.*, 2025, **43**, 1635–1647.
- 299 M. D. Komane, P. N. Kayoka-Kabongo and D. A. Rutkowska, *Viruses*, 2025, **17**, 218.
- 300 J. Langley, E. Pastural, S. Halperin, S. McNeil, M. ElSherif, D. MacKinnon-Cameron, L. Ye, C. Grange, V. Thibodeau, J. F. Cailhier, R. Lapointe, J. McElhaney, L. Martin, M. Bolduc, M. E. Laliberte-Gagne, D. Leclerc and P. Savard, *Vaccines*, 2020, **8**, 393.

